Biol Cybern
DOI 10.1007/s00422-006-0126-0

ORIGINAL PAPER

Biological Cybernetics

# A model of cerebrocerebello-spinomuscular interaction in the sagittal control of human walking

**Sungho Jo · Steve G. Massaquoi**

Received: 9 May 2006 / Accepted: 5 September 2006


**Abstract** A computationally developed model of human upright balance control (Jo and Massaquoi on Biol cybern 91:188–202, 2004) has been enhanced to describe biped walking in the sagittal plane. The model incorporates (a) non-linear muscle mechanics having activation level -dependent impedance, (b) scheduled cerebrocerebellar interaction for control of center of mass position and trunk pitch angle, (c) rectangular pulse-like feedforward commands from a brainstem/spinal pattern generator, and (d) segmental reflex modulation of muscular synergies to refine inter-joint coordination. The model can stand when muscles around the ankle are coactivated. When trigger signals activate, the model transitions from standing still to walking at 1.5 m/s. Simulated natural walking displays none of seven pathological gait features. The model can simulate different walking speeds by tuning the amplitude and frequency in spinal pattern generator. The walking is stable against forward and backward pushes of up to 70 and 75 N, respectively, and with sudden changes in trunk mass of up to 18%. The sensitivity of the model to changes in neural parameters and the predicted behavioral results of simulated neural system lesions are examined. The deficit gait simulations may be useful to support the functional and anatomical correspondences of the model. The model demonstrates that basic human-like walking can be achieved by a hierarchical structure of stabilized-long loop feedback and synergy-mediated feedforward controls. In particular, internal models of body dynamics are not required.

S. Jo (✉) · S. G. Massaquoi
Department of Electrical Engineering and Computer Science, Computer Science and Artificial Intelligence Laboratory, Laboratory for Information and Decision Systems, Massachusetts Institute of Technology, 32 Vassar St., Cambridge, MA 02139, USA
e-mail: shjo@csail.mit.edu

## 1 Introduction

Burgeoning interest in robot design and in human motor control and its disorders has stimulated computational investigations of natural upright balance and locomotion control. A range of studies have identified underlying patterns of kinematics and muscular activation (Anderson and Pandy 2001; Ogihara and Yamazaki 2001; Perteka 2003; Jo and Massaquoi 2004; Loram et al. 2004). Most have investigated the problems of balance and locomotion separately. Human postural balance has been studied and modeled chiefly with regard to postural disturbances or characteristics of natural sway (Jo and Massaquoi 2004; Perteka 2003; Kuo 1995; Johansson et al. 1988). These indicate that human-like balancing can be afforded by simple feedback circuitry. There have also been a number of models of physiological walking. Some have focused on the role of spinal pattern generators in the production of quadrupedal gait (Fukuoka et al. 2003; Kimura et al. 2001) where balancing requirements are important, but less demanding. Kimura and Fukuoka have constructed a quadruped walking robot "Tekken" whose control is based on biological concepts. The actuators are viscoelastic and its neural system model consists of neural pattern generators (NPGs) and vestibulospinal reflexes (Fukuoka et al. 2003). The NPG uses Matsuoka's equations to produce rhythmic joint motions. This nonlinear differential equation system models two tonically excited neurons with a self-inhibition, which are linked reciprocally via

inhibitory connections (Matsuoka 1987). A modified proportional type feedback control system representing the vestibulospinal reflex controls body roll and pitch angles. Peripheral feedback also affects the phase transitions in the NPG. Adjustable gains in the muscular control based on the phase of the NPG enables the robot to adapt to different walking speeds and to irregular terrain.

Bipedal walking places particular demand on integrating the control of balance and gait. Two neuromusculo-skeletal models of bipedal walking have been particularly successful. First, Taga's model (Taga 1995) includes eight body segments, ground contact elements, and 20 muscles. Its neural controller defines a sequence of global states in terms of body's center of mass (COM) and center of pressure (COP). Inputs from neural oscillators [using Matsuoka's equations (Matsuoka 1987)], located at each joint, are modulated by the neural controller in order to generate stable limit cycles. Low-level feedback control is afforded by impedance controllers that represent muscles. This mechanism generated stable gait in the sagittal plane. Secondly, the model of Ogihara and Yamazaki (2001) employs NPGs and, in comparison with Taga's mdoel, emphasizes detail in the actuation and peripheral neural feedback. The model defines muscles that include Hill-type force–length–velocity relationships, reflexes from muscle spindles, tendon organs, and foot tactile receptors. A genetic algorithm was used to find realistic walking motion. These models show that qualitatively realistic bipedal walking kinematics can be achieved using biomorphic components. However, these models have not demonstrated the capacity to walk at different speeds or to balance upright when stationary without changes in physical parameters. Also, the sensitivity to changes in physical characteristics and to disturbances has not been examined. Most of all, the nature of the higher levels of central nervous system control of bipedal gait remains essentially unexplored.

It has been shown that realistic control of upright balance can be accounted for in terms of stabilized long-loop (trans-cerebrococerebellar) proprioceptive and force feedback (Jo and Massaquoi 2004). This system affords energetic efficiency because muscular co-activation and associated active body stiffness can be reduced, It also affords flexibility and automaticity of response patterns because feedback gainsets can be modified according to sensed changes in body state. The model also manages robustly the potentially destabilizing effects of long-loop neural signal transmission delays and muscular excitation-activation phase lags that have not been heretofore included in neuromorphic locomotor control models. At the same time, considerable work on spinal physiology has shown that certain basic muscle activation patterns (synergies) may be coded within the cord (Tresch et al. 1999; d'Avella et al. 2003). Simulations of muscle synergies in a model of the frog hindlimb with simple switch-like commands have been shown to generate a range of movements consistent in both kinematics and muscle activations with real behaviors (Cajigas-González 2003). Thus, given the intimate relationship between upright balance and bipedal locomotion, and the wealth of physiological data that indicates important cerebral, cerebellar, brainstem and spinal roles in balance, patterned leg motion and locomotion, an integrated model describing the hierarchical neural control of both balance and walking appears valuable. In particular, it may be expected a priori that long-loop control may afford similar functional advantages to locomotor control as it does for standing balance. It may also be suspected that recruitable muscular synergies organized at a spinal level may help to reduce control demands upon higher level systems.

Ultimately, it is also of conceptual interest to determine the simplest formulation that is consistent with recognized functional anatomy. Fundamental questions include: What are the sufficient feedforward command variables? How complex must feedforward signals be to manage body dynamics during walking? What types of long-loop and segmental feedback processing are necessary and sufficient to support the basic feedforward motor command? What are possible roles of spinally organized muscle activation synergies and what is their relationship to central NPGs?

In this article, a basic model of Sagittal control of Bipedal Balance and Walking (SBBW) is proposed. It shows that long-loop responses, if stabilized and modulated by cerebrocerebellar interaction, can afford sufficient upright balance to allow basic walking to be driven at different speeds simply by adjusting the frequency and amplitude of two five-state rectangular pulse generators that engage four, potentially five, time-invariant muscular control synergies. Peripheral reflexes provide modulation that improves walking efficiency, and security, but are not fundamentally required for the basic gait pattern. Simulated lesions of the cerebellar and peripheral feedback systems give rise to certain control defects that are grossly similar to those observed clinically. This feature supports the model's proposed structure-function correspondences. On the other hand, certain features of experimentally observed muscle activation patterns are not predicted by the SBBW model. This indicates that there exist more than one muscle control pattern that are consistent with observed walking kinematics. The implications of this observation are discussed.

## 2 Neurophysiological background and principal modeling assumptions

### 2.1 Neural control of basic locomotor muscle activation patterns

A large number of systems potentially influence posture and gait including cerebral cortex (King 1927; Nielsen 2003; Dietz 1992), cerebellum (Dietz 1992; Morton and Bastian 2004; Mortan and Bastian 2003), basal ganglia including subthalamic locomotor region (Zijlstra et al. 1998; Shik and Orlovsky 1976; Dietz 1992), midbrain locomotor region (Grillner 1975; Shik and Orlovsky 1976; Kandel et al. 2000) and spinal cord with segmental reflexes (Duysens et al. 2000; Knikou et al. 2005; Brooke et al. 1997; Grillner 1975; Dietz 1992; Shik and Orlovsky 1976). Here a parsimonious mechanism is sought with the intention of identifying the minimal or near-minimal neural control requirements for human-like bipedal gait. At least in primates, upright walking appears to require the integrity of cerebral cortical control of legs, midline cerebellum including at least the fastigial nucleus (Mori et al. 2004) and possibly the interpositus (Amstrong and Edgley 1988), the brainstem and spinal cord. While basal ganglionic dysfunction leads to a host of walking deficits (Zijlstra et al. 1998; Kandel et al. 2000; Shik and Orlovsky 1976) it is not clear that explicit representation of basal ganglionic function is required to account for basic locomotion pattern. Certainly in a supported decerebrate cat, highly coordinated walking motions can be elicited by stimulation of cerebellar or mesencephalic centers (Grillner 1975; Mori et al. 1999; Shik and Orlovsky 1976; Kandel et al. 2000). So, for the purposes of this study, basal ganglia function will be taken to be subsumed within cerebrocrebellar interaction discussed below.

In any case, the impression of most investigators is that during locomotion, higher systems drive and modulate spinal level systems that are responsible for much of the basic patterning of muscle activity. The precise hierarchical partitioning of function has not yet been determined. However, several observations are relevant. (1) Muscular activation and leg function during locomotion (Ivanenko et al. 2004) indicate that the electromyogram (EMG) pattern is consistent across movement speeds, with only duration and intensity changing (inversely). Several investigations (Ivanenko et al. 2004, 2005, Davis and Vaughan 1993; Olree and Vaughan 1995) have used factor and principal component analysis, and nonnegative matrix factorization to decompose to such activity into a combination of four or five principal waveforms, most of which have only modest, but not zero temporal overlap. (2) Experimental observations support a spinal locus for important rhythmic locomotor EMG pattern generation in humans (Dimitrijevic et al. 1998; Grasso et al. 2004; Calancie et al. 1994; Dietz and Harkema 2004) often in response to tonic electrical stimulation (Dimitrijevic et al. 1998). (3) Experimental stimulation of either the cerebellum or midbrain produces rhythmic locomotor movement in both intact and decerebrate cat with vigor and frequency that increase with stimulus intensity (Mori et al. 1998, 1999). These locomotor regions both strongly recruit vestibulospinal, reticulospinal and other direct spinal efferent pathways (Shik and Orlovsky 1976). A parsimonious proposition is that the cerebellar and midbrain locomotor regions can each drive and potentially modulate a spinal locomotor control system consistent with previous suggestions (Grillner 1975; Mori et al. 1998, 1999; Kandel et al. 2000; Shik and Orlovsky 1976). (4) Tonic stimulation of frog spinal cord demonstrates synergistic patterns of muscle activities (Tresch et al. 1999; Cheung et al. 2005; d'Avella et al. 2003; d'Avella and Bizzi 2005). Such a mechanism collapses multiple muscle control into lower degree-of-freedom control for each leg. The lower dimensional representation can still account for a wealth of frog leg EMG activities and behaviors including wiping, crawling and swimming (Cajigas-González 2003).

These findings suggest that a rhythmic central pattern generator, modulated from above, may interact with muscle control synergies to provide a simple and effective walking control. Numerous studies indicate the complexity of segmental spinal cord circuitry (Rossignol et al. 2006; Grillner 1975; Brooke et al. 1997), which will not be modeled explicitly here. Rather, a simple representation of spinal control has been sought that may be functionally equivalent to the actual system under the restricted, but important condition of moderate velocity forward walking with modest push disturbances. In particular, here it will be examined whether basic walking can be driven by four or five *sequential*-rectangular pulses during the gait cycle for each leg. At the level of the spinal pulse generator, locomotor function will be therefore viewed in terms of five hypothetical *control epochs*: "loading" (LOA), "regulation" (REG), "thrust" (THR), "retraction" (RET) and "forward" (FOW) (Fig. 4). The last is almost, but not precisely coextensive with actual swing phase. Plausibly, these five phases may be driven at a range of frequencies. Sequential, multi-state transitioning appears to be consistent with simple physiological oscillator models studied by Iwasaki and Zheng (2006). Other proposed multi-state oscillator implementations include pairs of half-center oscillators (Fukuoka et al. 2003) and a symmetric ring of $n$ coupled nonlinear oscillators

(Collins and Stewart 1994). Although a priori it is not necessary that the relative durations of each control epoch remain fixed, this is the simplest assumption and will be adopted here. If the output intensities of such a pulse generator were scaled appropriately with frequency, effective muscle activation might be afforded by linear combinations of independently recruitable muscle activation patterns, or time-invariant *control synergies* (e.g. Cajigas-González 2003). We note here that the term "synergy", while generally used to refer to task-related groupings of multiple muscle activities, may have a variety of interpretations. For specificity and consistency with a motor control perspective, the term *time-invariant control synergy* is used herein to specify a linear distribution of a single control signal into multiple command signals that are directed to a set of muscles. This distribution will be represented by columns within signal distribution matrix. The total EMG will then be determined by the superposition of several operative control synergies. Each control synergy vector is considered time-invariant in the sense that any change or adaptation of its elements is assumed to occur at a time scale vastly slower than any individual movement. All moment-to-moment variation in command signal intensity is therefore attributed to variation in the control input signal, and/or the selection or "recruitment" of different existing distribution matrices. The combination of the cyclic pulse generator and the linear distribution matrix will be referred to as a spinal locomotor pattern generator.

Other experiments have pointed out the role of peripheral neural input in modulating the locomotor pattern. The most important influences appear to be: (a) detection of ground contact (Rossignol et al. 2006; Nielsen 2003; Duysens et al. 2000; Zehr and Stein 1999), (b) the monitoring of hip angle which appears to be associated with releasing or triggering the forward step transition (thrust to retraction, in Fig. 4) (Knikou et al. 2005; Kriellaars et al. 1994; Duysens et al. 2000), (c) the peripheral position-dependent modulation of segmental reflexes (Baxendale and Ferrell 1981; Brooke et al. 1997; Duysens et al. 2000; Rossignol et al. 2006). It is known that presynaptic inhibition contributes to position-dependent modulation during locomotion (Duysens et al. 2000; Brooke et al. 1997; Stein 1995). Presynaptic inhibition refers to a depression of monsynaptic excitatory potentials that occurs in the absence of any postsynaptic potential change or any change in motoneuronal excitability (Rudomin and Schmidt 1999). This paper uses a simple model of the presynaptic inhibition to implement the position-dependent modulation at spinal cord level (see Sect. 3.2.1).

### 2.2 Cerebrocerebellar control of COM and trunk pitch

Without the cerebrum and cerebellum, the locomotor patterns are much simpler than normal stepping (Kandel et al. 2000). The cerebellum is critical for balance and studies have shown that selective lesions of descending control from the motor cortex compromise irrevocably certain fine control of especially swing leg trajectory in the cat (Drew 1993). The motor cortex also has been shown to contribute to structure and timing of step cycle during locomotion in the intact cat (Bretzner and Drew 2005). In humans, where fine integration of bipedal balance and stepping must be exquisite, disconnection of cerebral control of legs due to stroke or tumor yields devastating effects in postural balance and locomotion (Porter and Lemon 1993). Thus, normal bipedal function in humans appears to depend significantly upon activity in transcerebral pathways (Nielsen 2003; Peterson et al. 1998; Nathan 1994). Moreover, it has been noted that most of cerebral activity during locomotion appears to be generated by sensory afferent feedback (Christensen et al. 2000; Nielsen 2003) which suggests a prominent role for long-loop feedback mechanisms. For these reasons, the modeling here as did that in upright balance control (Jo and Massaquoi 2004) includes at least a rudimentary trans-cerebrocerebellar feedback loop.

The control of sagittal planar upright posture during walking is similar to that exerted during stationary balance except that it is potentially more intermittent and/or weaker in the sense that the upper body generally remains close to vertical in both situations so that trunk posture can help to control the body's COM within a supporting area (Gilchrist and Winter 1997). It is natural therefore to consider beginning with the upright balance model explored previously by the authors [FRIPID model, (Jo and Massaquoi 2004)]. Still, it is possible to walk or even run with the trunk bent forward or backward. And during running, the trunk is maintained erect even while there is no ground contract and the legs are not vertical. Therefore, it is plausible that regulation of trunk pitch and COM position relative to the leg configurations are managed by separate circuits. This is consistent with recent experimental work by Freitas et al. (2006) and appears to be a necessary model extension. The FRIPID model showed that smooth switching or scheduling cerebellar gains associated with proportional-integral-derivative (PID) control circuits as a function of sensed body state enabled the cerebrocerebellar system to automatically modify its responses according to disturbance strength. The switching system was argued to be easily compatible with

known cerebellar cortical microcircuitry. Importantly, interpolation between just two gainsets was sufficient to account for the full range of balancing strategies. Similarly, the current model considers the possibility that a single or small set of cerebellar gains would also be sufficient for walking control.

The availability of spinal synergies also enables an important simplification of the cerebellar control in the SBBW model with respect to that proposed in the FRIPID model (Jo and Massaquoi 2004). Under the assumption that certain signals ascending the spinal cord e.g. via spinocerebellar tracts, may consist of linear combinations of proprioceptive information (see Jo and Massaquoi 2004; Osborn and Poppele 1992), the presence of synergies in the efferent path allows multiple joints to be both sensed and controlled by single cerebellar modules. Specifically, one single-input single-output (SISO) cerebellar channel can engage a synergy that spans ankle, knee and hip to control the trunk and stance. This could simplify tracking of the intended COM position as specified in the cerebral cortex. An independent SISO channel can engage muscles at the hip to control trunk pitch relative to vertical based on vestibular input and/or ankle, knee and hip angles, together with an assumed pitch for the stance surface. Such decoupling is similar to that used recently to control robotic locomotion (Hofmann 2006). Hence, in the SBBW model, cerebellar balance control is implemented by $2 \times 2$ diagonal matrices instead of fully populated $3 \times 3$ matrices as used in Jo and Massaquoi (2004) (see Sect. 5.6). On the other hand, the SBBW model is not designed to account for all features of human upright balancing such as postural strategies (Jo and Massaquoi 2004) because the model focuses on walking.

### 2.3 Summary of principal physiological modeling assumptions

In summary, the SBBW model assumes:

(PA-1) The feedforward action of brainstem and spinal cord in locomotor muscle patterning can be summarized as a five-state activation/relaxation process that drives time-invariant muscle activation synergies. This process controls the intensity and frequency of synergy activation.

(PA-2) The influence of peripheral input can be considered to consist most importantly of (a) an indication of which leg is in contact with the ground, (b) a modulation of synergies to improve step morphology by altering a spinal muscle activation threshold via presynaptic inhibition.

(PA-3) The control afforded by the cerebrocerebellar long-loop circuitry is implemented by three independent channels. One operates continuously to regulate trunk verticality, and two others represent independent, parallel control of respectively left and right leg postures at stance needed to regulate intended relative COM position. Detection of ground contact (PA-2a) is used to gate trans-cerebellar long-loop COM control to the supporting leg (Duysens et al. 2000; Nielsen 2003; Zehr and Stein 1999; Morton and Bastian 2003).

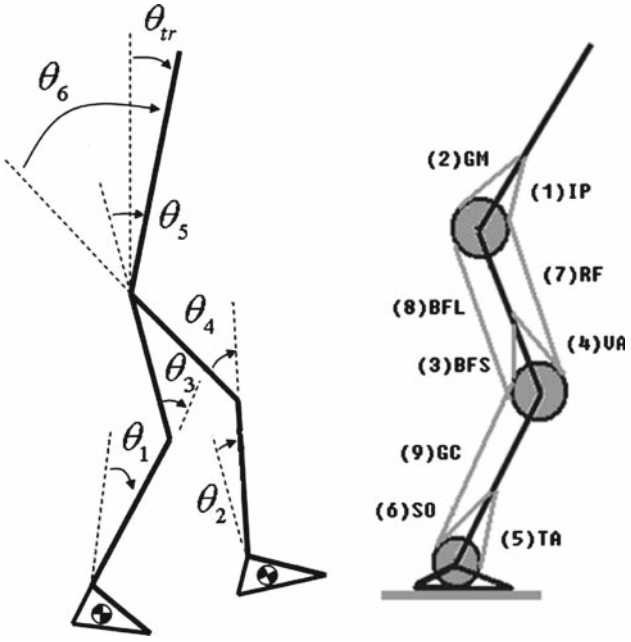


**Fig. 1** (*Left*) Body configuration joint angle convention: $\theta_1, \theta_3, \theta_5$ are respectively ankle, knee, and hip angles for right leg, and $\theta_2$, $\theta_4$, $\theta_6$ ankle, knee, and hip for left leg. $\theta_{tr}$ is the trunk pitch angle. Arrows indicate directions where angle values increase. (*Right*) Muscle diagram (one leg for simplicity) with muscles identified in Table 2

## 3 Methods

### 3.1 Spinomusculoskeletal plant model

#### *3.1.1 Skeletal system and ground contact*

A seven-segment kinematic chain with pivot joints was used to represent human walking in the sagittal plane (Fig. 1). Positive angular motion was consistent with anatomical flexion at the hip and knee, and dorsiflexion at the ankle. Each leg incorporates nine muscles.

The length of each segment is represented with respect to the total body's height $H_B$ (Fig. 2a). Each segment's mass and moment of inertia are calculated with respect to $H_B$ and the body's mass $M_B$ in Table 1. The position of center of mass at feet is detailed in Fig. 2b.

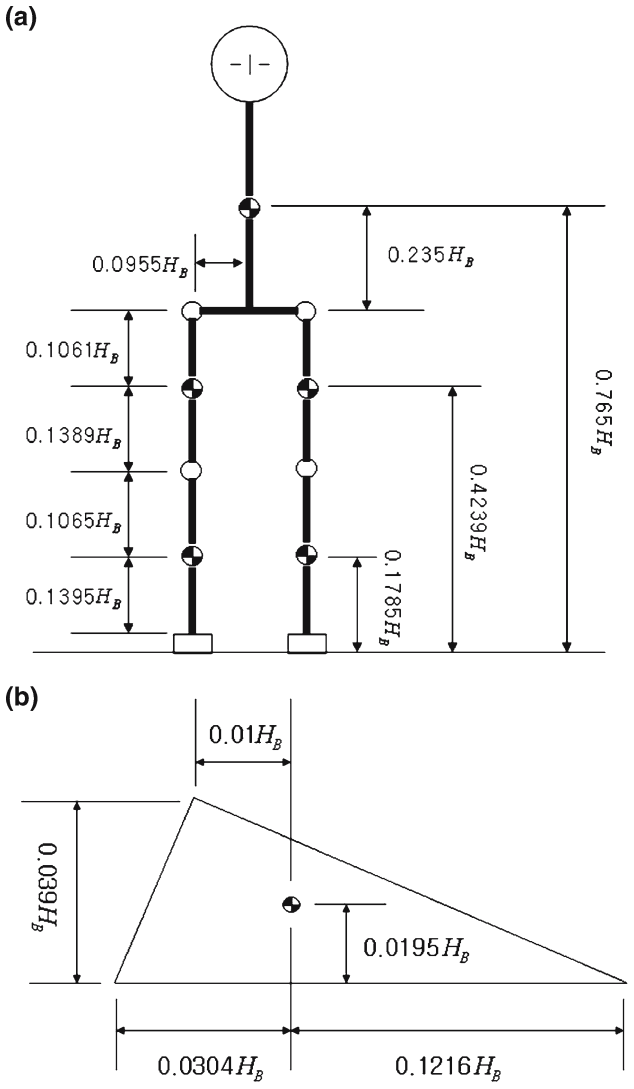


**Fig. 2** **a** Body segment length and **b** foot dimensions (Winter 1990). Centers of component masses are indicated by small checkered discs

The natural locking of the knee that prevents hyperextension is modeled by a high impedance damped elasticity:

$$\tau_{i,\text{lock}} = \begin{cases} \max(K_k(\theta_{i,\min} - \theta_i) - B_k\dot{\theta}_i, 0) & \text{if } \theta_i < \theta_{i,\min} \\ \min(K_k(\theta_{i,\max} - \theta_i) - B_k\dot{\theta}_i, 0) & \text{if } \theta_i > \theta_{i,\max} \end{cases} \tag{1}$$

where $K_k$, $B_k$ are, respectively, spring and damper coefficients, $\theta_{i,\min}$ is a minimum knee angle, and $\theta_{i,\max}$ is a maximum knee angle, and $\theta_i$ is an actual knee angle. For this research, $\theta_{i,\min}$ is set to be $-160$ degrees, and $\theta_{i,\max}$ to be zero degree.

The body model's dynamics in response to applied total muscular and ground reaction torques applied to the joints, $\tau_M(\Theta, \dot{\Theta}, \text{act})$ and $\tau_R(F_{gx}, F_{gy}, \Theta)$ , respectively, is given by

$$H(\Theta)\ddot{\Theta} + C(\Theta, \dot{\Theta}) = \tau_M(\Theta, \dot{\Theta}, \text{act}) + \tau_R(F_{gx}, F_{gy}, \Theta) + G(\Theta) \tag{2}$$

where $\Theta = \begin{bmatrix} \theta_1 & \theta_2 & \theta_3 & \theta_4 & \theta_5 & \theta_6 \end{bmatrix}^{\mathrm{T}}$, $\dot{\Theta} = \begin{bmatrix} \dot{\theta}_1 & \dot{\theta}_2 & \dot{\theta}_3 & \dot{\theta}_4 & \dot{\theta}_5 & \dot{\theta}_6 \end{bmatrix}^{\mathrm{T}}$, and $\text{act} = [act_1 \ act_2 \cdots act_9]^{\mathrm{T}}$ represents the muscle activations defined below (Eq. 11), $H(\Theta)$ is the symmetric configuration-dependent body inertia matrix, $C(\Theta, \dot{\Theta})$ is the matrix related to centrifugal and Coriolis forces, $G(\Theta)$ is the gravitational effect matrix, and $\tau_R(F_{gx}, F_{gy}, \Theta)$ is the torque generated by horizontal and vertical reaction forces to the ground at heel and toe (the details in section ). The dynamics are executed using SimMechanics in Matlab (MathWorks Inc., Natick, MA, USA).

### *3.1.2 Muscle structure and activation*

Muscular torque is determined by the total muscular force (passive + active) $\mathrm{F}(\mathrm{l}, \dot{\mathrm{l}}, \text{act})$ and the moment arms of each muscle according to

$$\tau_M(\Theta, \dot{\Theta}, \text{act}) = a^T F(\mathrm{l}, \dot{\mathrm{l}}, \text{act}) \tag{3}$$

$$\mathrm{A}^{\mathrm{T}} = \begin{bmatrix} 0 & 0 & 0 & 0 & -a_5 & a_6 & 0 & 0 & a_9^a \\ 0 & 0 & a_3 & -a_4 & 0 & 0 & a_7^k & -a_8^k & -a_9^k \\ -a_1 & a_2 & 0 & 0 & 0 & 0 & -a_7^h & a_8^h & 0 \end{bmatrix} \tag{4}$$

where $a_i^{jo}$ is the estimated average moment arm over the usual range of motion of the $i$th muscle in Table 2. $jo = a, k$, or, $h$ to distinguish ankle, knee and hip joint moment arms, respectively, in biarticular muscles. Flexor moment arms are negative reflecting the relationship between length change and direction of rotation.

The model views the anatomically redundant muscles of the trunk and legs as operating together as functional groups of uni- and biarticular flexors and extensors as shown in Fig. 1. Assuming that stiffness is proportional to physiological cross-sectional area (PCA) (Brand et al. 1986), the relative muscle stiffness scaling is given based on morphmetric data in Table 2.

Passive muscular force is expressed by

$$\mathrm{F}_{pass} = \left[\mathrm{K}_{pass}(\mathrm{l}_{eq} - \mathrm{l}) - \mathrm{B}_{pass}\dot{\mathrm{l}}\right]_+ \tag{5}$$

where $[x]_+ = \begin{cases} x, & x > 0 \\ 0, & x \le 0 \end{cases}$, $\mathrm{F}_{pass}$ is passive tension vector, $\mathrm{K}_{pass}, \mathrm{B}_{pass}$ passive muscle stiffness and viscosity

**Table 1** Body segment's masses and moments of inertia calculated based on Winter (1990)

| Body physical parameters | | | | |
|---|---|---|---|---|
| | Body segment, $H_B = 1.8\,\mathrm{m}$, $M_B = 80\,\mathrm{kg}$ | | | |
| | Trunk | Upper leg | Lower leg | Foot |
| Mass (kg) | $0.678M_B$ | $0.1M_B$ | $0.047M_B$ | $0.015M_B$ |
| Moment of inertia ($\mathrm{kg\,m^2}$) | $0.031M_BH_B^2$ | $6.262\times10^{-4}M_BH_B^2$ | $2.566\times10^{-4}M_BH_B^2$ | $4.976\times10^{-6}M_BH_B^2$ |

matrices, $\mathrm{l}_{eq}$ is muscle length vector at equilibrium, l is actual muscle length vector. Active muscular force as a function of neural input to each muscle (act ) is represented by

$$\mathrm{F}_{act} = \mathrm{K}_{act}(\mathrm{act})[\mathrm{l}(\mathrm{act}) - \mathrm{l}]_+ - \mathrm{B}_{act}(\mathrm{act})\dot{\mathrm{l}} \tag{6}$$

where $\mathrm{F}_{act}$ is active tension vector, $\mathrm{l}(\mathrm{act}) = \mathrm{l}_{eq}+\mathrm{act}$. $\mathrm{K}_{act}(\mathrm{act})$, and $\mathrm{B}_{act}(\mathrm{act})$ are the active muscle stiffness and viscosity matrices which are functions of muscular activation.

$$\begin{aligned}\mathrm{K}_{act}(\mathrm{act}) &= \mathrm{K}_a\left(\alpha[\mathrm{act}]_+ + \beta\min(\gamma[\mathrm{act}]_+, 1)\right)\\ \mathrm{B}_{act}(\mathrm{act}) &= \mathrm{B}_a\left(\alpha[\mathrm{act}]_+ + \beta\min(\gamma[\mathrm{act}]_+, 1)\right)\end{aligned} \tag{7}$$

where $\mathrm{K}_a$, $\mathrm{B}_a$ are constant matrices, and $\alpha$, $\beta$, and $\gamma$ are constant coefficients. When both passive and active tensions are applied together,

$$\mathrm{F}(\mathrm{l}, \dot{\mathrm{l}}, \mathrm{act}) = \left[F_{pass}(\mathrm{l}, \dot{\mathrm{l}}) + F_{act}(\mathrm{l}, \dot{\mathrm{l}}, \mathrm{act})\right]_+ \tag{8}$$

$$\mathrm{l} = \mathrm{l}_{eq} + \mathrm{A}(\Theta - \Theta_{eq}) \tag{9}$$

where $\Theta$ is joint angle vector at equilibrium.

The positive brace means that each muscle is constrained to exert only contractile force. This formulation substantially follows that employed by Katayama and Kawato (1993). The effective pre-set (e.g. before reflex neural activation) rotational stiffness of the ankle during standing is about 90 Nm/rad (Fujita and Sato 1998). This value was used to determine the absolute passive stiffness of each muscle given their relative scaling which is proportional to the cross-sectional area in Table 2. It was assumed that $\mathrm{K}_a = 2.5\mathrm{K}_{pass}$ and $\mathrm{B}_a = 2.5\mathrm{B}_{pass}$. $\alpha[\mathrm{act}]_+ + \beta\min(\gamma[\mathrm{act}]_+, 1) < 1$ holds over simulations, therefore, active stiffness is maximally less than 250% of passive stiffness and damping ratio could approximately increase up to 50% because the ratio is proportional to $B/\sqrt{K}$. This was considered based on human arm modeling study where stiffness and damping ratio have been shown to increase up to 500% and 50%, respectively (Lacquaniti and Soechting 1986), with strong activation. In general, magnitude of muscle viscosity was set at one-tenth that of the muscle stiffness as has been done in arm modeling (Flash 1987).

The activation of muscle force by neural input occurs according to low-pass dynamics that can be approximated by the filter with Laplace transfer function:

$$EC(s) = \frac{\rho^2}{(s+\rho)^2}, \quad \rho = 30\,\mathrm{rad/sec} \tag{10}$$

**Table 2** Length, moment arm, and physiological cross-sectional area (PCA) parameter values of muscles determined from Ogihara and Yamazaki (2001), and Winter (1990)

| Muscle | Location | $l_{eq}$ (m) | $a_i^{jo}$ (m) | PCA ($\mathrm{cm^2}$) |
|---|---|---|---|---|
| Iliopsoas (IP) | mono, hip flexor | 0.35 | 0.132 | 17 |
| Gluteus Maximus (GM) | mono, hip extensor | 0.30 | 0.092 | 30.4 |
| Rectus femoris (RF) | bi, hip flexor, knee extensor | 0.48 | 0.049($h$), 0.025($k$) | 12.5 |
| Biceps femoris long (BFL) | bi, knee flexor, hip extensor | 0.46 | 0.054($h$), 0.049($k$) | 15.8 |
| Vastus (VA) | mono, knee extensor | 0.26 | 0.04 | 30 |
| Biceps femoris short (BFS) | mono, knee flexor | 0.29 | 0.049 | 6.8 |
| Tibialis anterior (TA) | mono, ankle dorsiflexor | 0.30 | 0.023 | 9.1 |
| Gastrocnemius (GC) | bi, knee flexor, ankle plantarflexor | 0.56 | 0.050($k$), 0.040($a$) | 30 |
| Soleus (SO) | mono, ankle plantarflexor | 0.35 | 0.036 | 58 |

(Fuglevand and Winter 1993) where $s$ is the Laplace variable, and then

$$\text{act} = EC(s)\,(\text{u}_\alpha) \tag{11}$$

meaning that the filter is applied to $\text{u}_\alpha$ that is the alpha motor neuronal output.

The dynamics of series elasticities, filtering action of spindles, segmental proprioceptive and force feedback, and spinal processing by alpha motorneuron — Renshaw cell networks were not modeled explicitly, although it is likely that these could improve the accuracy of the simulations (Winters 1995). However, it was not felt that these features would bear significantly upon the basic neuromuscular mechanisms of gait control.

### *3.1.3 Foot interaction with the ground*

When the heel or toe contacts the ground, horizontal and vertical reaction forces are typically generated (Fig. 12). During $(y_{gy}(x^i) > y^i)$, vertical reaction force is modeled by

$$F^i_{gy} = \left(K_{gy}\left(y_{gy}\left(x^i\right) - y^i\right) - B_{gy}\dot{y}^i\right) \tag{12}$$

where $(x^i, y^i)$ indicates the positions of either heel or toe with $i = heel, toe$. $y_{gy}\,(x^i)$ represents the ground profile as a function of $x^i$. $K_{gy}$ and $B_{gy}$ are coefficients. $F^i_{gy}$ is always nonnegative. The horizontal reaction force is modeled in two ways.

During contact, the horizontal reaction force is modeled by a spring and damper system as long as the horizontal reaction force is smaller than the maximal friction force ($|F^i_{gx}| \leq |\mu_s F^i_{gy}|$ where $\mu_s$ is the static frictional coefficient).

$$F^i_{gx} = \left(K_{gx}\left(x^i_o - x^i\right) - B_{gx}\dot{x}^i\right) \tag{13}$$

where $x^i_o$ is a location where either heel or toe touches the ground initially and $K_{gy}$ and $B_{gy}$ are coefficients.

However, if the horizontal reaction force is larger than the maximal friction force ($|F^i_{gx}| > |\mu_s F^i_{gy}|$), Eg. 14 represents the horizontal reaction force.

$$F^i_{gx} = -\mu_k F^i_{gy}\text{sgn}(\dot{x}^i) \tag{14}$$

where $\mu_k$ is the dynamic frictional coefficient.

As as result, the total vertical and horizontal reaction forces between foot and ground are respectively:

$$F_{gy} = F^{toe}_{gy} + F^{heel}_{gy}, \quad F_{gx} = F^{toe}_{gx} + F^{heel}_{gx}. \tag{15}$$

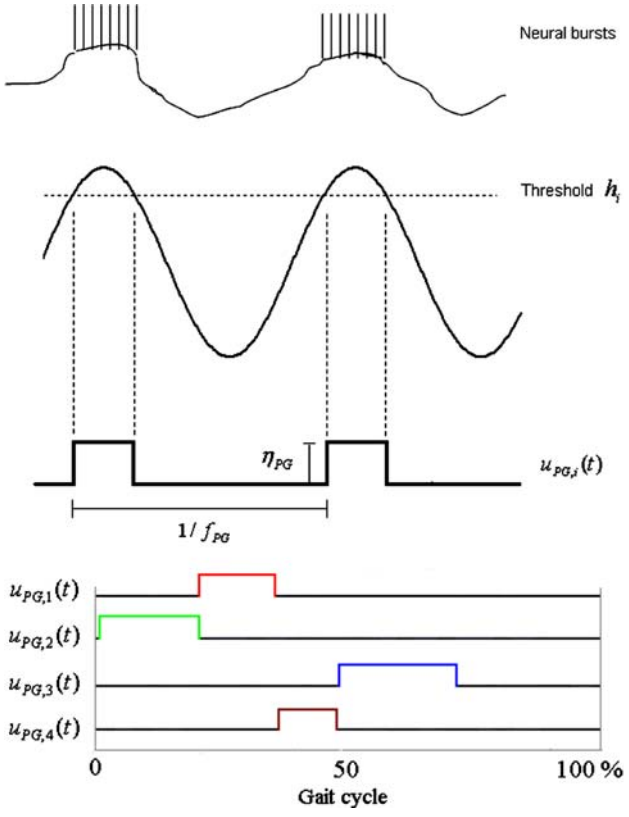


**Fig. 3** Periodic spinal command pulse generation. *Top* Schematic representation of the membrane potential of a hypothetical neuron within an oscillating circuit. Action potential pikes representing output are fired when a threshold is crossed, and firing rate (intensity) is modeled by a rectangular pulse that occurs when threshold is traversed. *Bottom* The spinal pulse output commands are summarized

## 3.2 Central neural control model

### *3.2.1 Spinal pulse generator and locomotor control synergies*

Many models of central pattern generators have been considered (Matsuoka 1987; Patla et al. 1985; Iwasaki and Zheng 2006; Collins and Stewart 1994). For the present purposes, it is sufficient to consider a five-state machine whose states transition in a strict, fixed sequence. Each state is comparable with each control epoch. For simplicity and generality, the state machine will be considered to have scaled binary output that is processed by a linear signal distribution matrix. The command output of each state register is designated $u_{PG,i}(t)$. As a further simplification, the command output of the fifth state register, $u_{PG,5}(t)$, is intentionally set to zero to correspond to an almost completely passive swing phase of each leg.

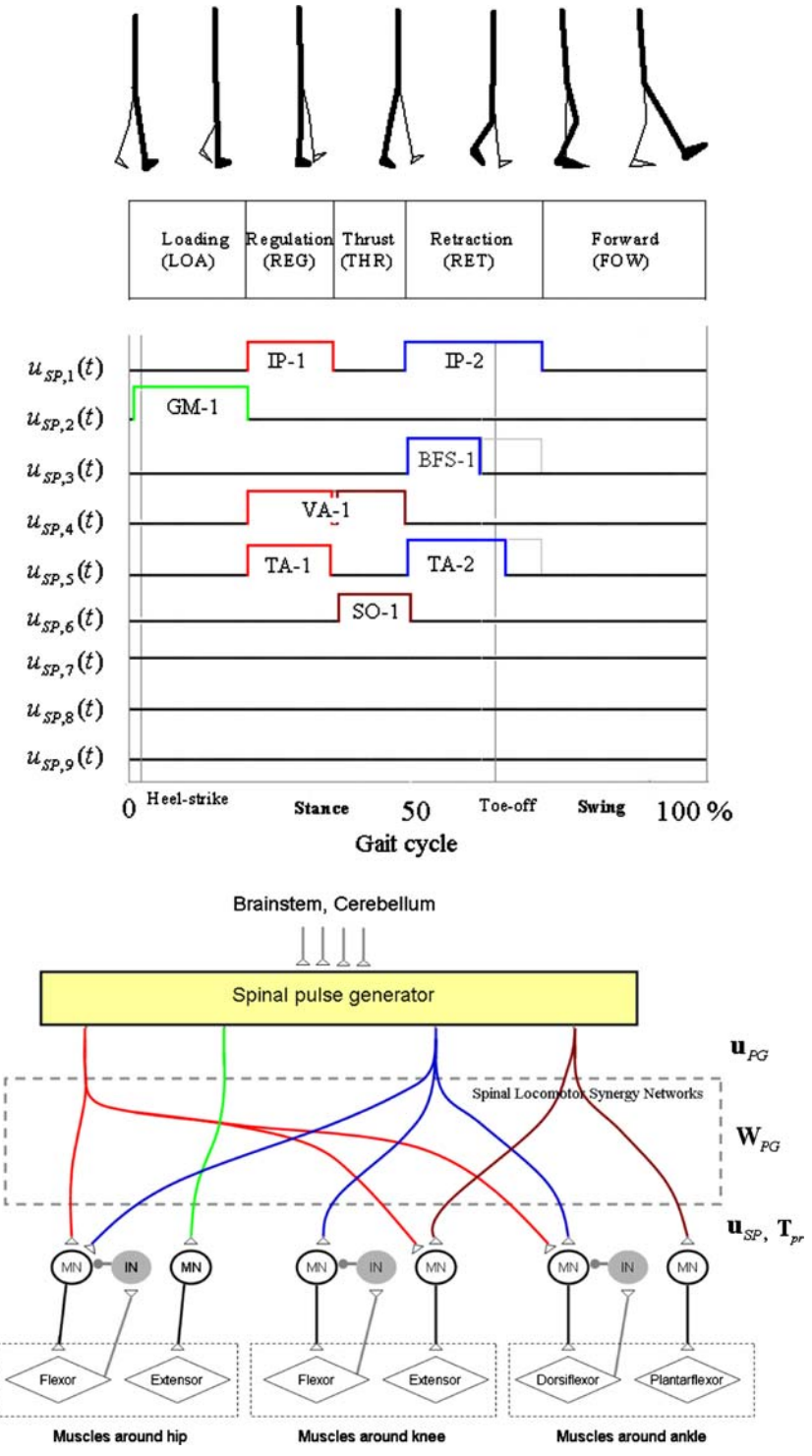


**Fig. 4** Decomposed spino-locomotor signals and a model of the locomotor control synergy network. *Top* Proposed control epochs and spinally generated command by muscle and phase of gait. *Shaded lines* indicate suppressions by presynaptic inhibition. *Bottom* Hypothetical model of connection between pattern generator and muscle. Neural signals are subsequently delayed as much as $\mathrm{T}_{pr} = \left[\, T_{pr,a} \quad T_{pr,k} \quad T_{pr,h} \,\right]^{\mathrm{T}}$

As in Fig. 3, for $i = 1, \ldots, 4$, its periodic activation can be modeled as

$$u_{PG,i} = \eta_{PG} \cdot 1\left[\cos(2\pi f_{PG} t - \phi_i) - h_i\right]_+ . \tag{16}$$

where $1[x]_+ = \begin{cases} 1 \text{ where } x > 0 \\ 0 \text{ where } x \leq 0 \end{cases}$, $f_{PG}$ determines the pattern frequency, $\eta_{PG}$ is an activation intensity factor, $\phi_i$ is the phase shift, and $h_i$ activity discharge threshold. Specification of $\phi_i$ and $h_i$ determines the sequence and potential overlap between the state activations. The values used in simulation are given in Table A-1 in Appendix B. The values of $\phi_i$ and $h_i$ were chosen to yield (a) no command overlap, (b) empirically most realistic gait patterns subject to constraint (a). Two identical pulse generators were used, one for each leg. A phase

difference of 180 degrees between the generators was enforced artificially as gaits other than simple walking were not entertained in this study.

It is proposed that pulse generator commands $\mathrm{u}_{PG} = \left[u_{PG,1}\ \ u_{PG,2}\ \ u_{PG,3}\ \ u_{PG,4}\right]^{\mathrm{T}}$ are distributed to the muscles according to a spinal locomotor control synergy network represented by the matrix $\mathrm{W}_{PG}$ (Fig. 4 and Appendix A) according to five functional tasks during the gait cycle. The fifth task, active control of swing leg, is, for the moment, ignored as mentioned above.

$$\mathrm{u}_{SP} = \mathrm{W}_{PG}\mathrm{u}_{PG} \tag{17}$$

The combination of spinal pulse generator and control synergy distribution matrix is considered an NPG. To develop a minimal model, synergies involving the monoarticular muscles alone were formed. Thus, the spinal activations $u_{SP,j}(t)$ are defined for $j = 1, ..., 6$ in Eq. 17 and Fig. 4. The signals for $j = 7, 8, 9$ were set to be zero. As discussed later, simulation of simple walking does not require biarticular muscle activation.

Each rhythmic spinally generated muscle command $u_{SP,j}(t)$ is thus a train of rectangular pulses (Fig. 4, *Top*). The primary function of each pulse is approximately to:

- IP-1: prevent the upper body from falling backward.
- IP-2: raise leg and trigger forward swing around hip.
- GM-1: prevent the upper body from forward rotation just after heel strike.
- BFS-1: help swing leg avoid ground contact by flexing knee.
- VA-1: maintain body support on stance leg by extending knee at mid-stance.
- TA-1: help COM move forward to insure step size.
- TA-2: help swing leg avoid ground contact by dorsiflexing ankle.
- SO-1: provide forward thrust using stance leg.

As detailed in the results, it was assumed that a separate additional pulse could be delivered (superposed on other commands) to IP to launch walking from a standing start. The physiological basis of such a pulse is not specified. However, as discussed below, it may be of cerebral origin.

Finally, the SBBW model proposes that peripherally triggered spinal inhibition can help to modify certain synergy components. One possible neural circuit involves presynaptic inhibition (Baxendale and Ferrell 1981; Brooke et al. 1997; Rossignol et al. 2006; Duysens et al. 2000) as shown in Fig. 4 and in greater detail in Fig. 5. A descending signal conveys a tonic excitation $\theta_{th,jo}$, $jo = a, k, h$(ankle, knee, hip), that inhibits

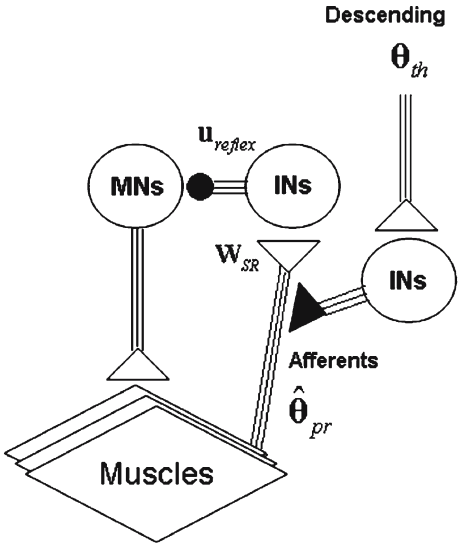


**Fig. 5** Presynaptic inhibition: depolarization of an afferent terminal (presynaptic inhibition) is indicated by the *filed triangle* ending on afferent pathway, inhibitory effect by the *filled circle*. MN: motorneuron, IN: interneuron

the proprioceptive afferent $\theta_{jo}$ until superseded. Thereafter, the interneuron is activated and the motor neuron activity is suppressed. It is speculated here that such a mechanism could truncate BFS-1 and TA-2 activity in early FOW to prevent excessive leg retraction. This mechanism is empirically useful to improve the timing between knee and ankle motions to prevent ground contact during swing phase. The spinal reflex action is therefore modeled as

$$\mathrm{u}_{reflex} = -\mathrm{W}_{SR} \cdot 1\left[\hat{\theta}_{pr} - \theta_{th}\right]_{+} \tag{18}$$

where $\theta_{th} = \left[\theta_{th,a}\ \theta_{th,k}\ \theta_{th,h}\right]^{\mathrm{T}}$, $\hat{\theta}_{pr} = \left[\theta_a(t - T_{pr,a})\ \theta_k(t - T_{pr,k})\ \theta_h(t - T_{pr,h})\right]^{\mathrm{T}}$ where $T_{pr,jo}$, $jo = a, k, h$, are unidirectional peripheral neural transmission delays from the spinal cord to the anke, knee and hip, respectively and $\mathrm{W}_{SR}$ is a $9 \times 3$ matrix that scales and distributes joint-related signals from the uniarticular muscles to the other muscles via the 9 element vector $\mathrm{u}_{reflex}$.

### 3.2.2 Suprasegmental control

The second component of the central neural control system modeled consists of two long-loop feedback pathways that add stability. The first is concerned with tracking the intended forward position of the body's COM relative to the stance foot as specified by the tonic reference signal $x_{com,ref}$. The second concerns maintaining the trunk-head segment close to vertical at all times. The pitch angle of the trunk-head segment is repre-

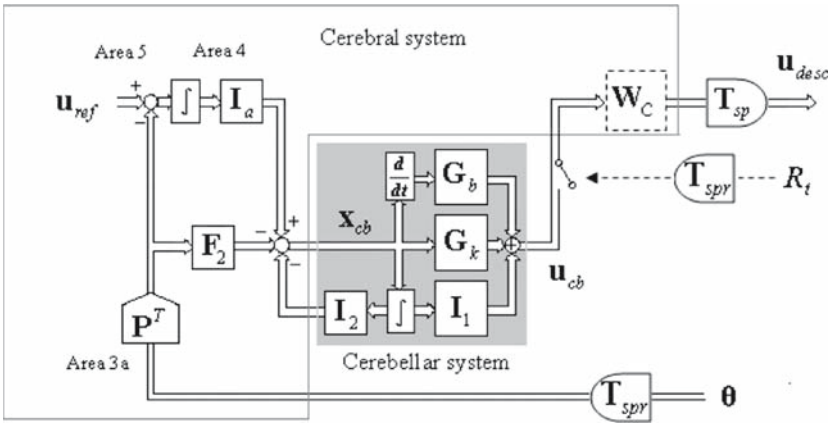


**Fig. 6** The RIPID cerebro-cerebellar control model applied to locomotor control

sented as $\theta_{tr}$ (Fig. 1) and therefore its intended position is $\theta_{tr,ref} = 0$. The cerebrocerebellar control model (Fig. 6) is simplified from Jo and Massaquoi (2004) in that a high speed "catching" gainset and force feedback are not employed. This is because the SBBW is not designed to cope with rapid foot slippage or translation of the support surface. Physiologically, it is also quite possible that important long-loop feedback control operates via sub(cerebral)cortical levels. However, from the perspective of managing long signal transmission delays the most challenging possibility is if significant processing occurs via trans(cerebral) cortical loops as it does in arm control. For conservatism, therefore, trans(cerebral) cortical long-loop feedback is modeled.

During simulated walking $x_{com,ref} = 25$ cm and this is compared to a linear estimate of COM position relative to the stance foot computed as

$$\hat{x}_{com} = p_{11}\theta_a(t - T_{spr,a}) + p_{21}\theta_k(t - T_{spr,k}) + p_{31}\theta_h(t - T_{spr,h}) = \mathrm{p}_1^T\hat{\theta}_{spr} \tag{19}$$

where $\mathrm{p}_1 = \begin{bmatrix} p_{11} & p_{21} & p_{31} \end{bmatrix}^{\mathrm{T}}$ are constants, and $\hat{\theta}_{spr} = \begin{bmatrix} \theta_a(t - T_{spr,a}) & \theta_k(t - T_{spr,k}) & \theta_h(t - T_{spr,h}) \end{bmatrix}^{\mathrm{T}}$. $\mathrm{T}_{spr} = \begin{bmatrix} T_{spr,a} & T_{spr,k} & T_{spr,h} \end{bmatrix}^{\mathrm{T}}$ are the afferent signal transmission delays including spinal and peripheral components. The scaling factors $p_{i1}$ were obtained by linearizing trigonometric relationships and neglecting contributions of the swing leg, as detailed in Appendix A.

The estimate of $\theta_{tr}$ is presumed to depend upon a similar linear estimate:

$$\hat{\theta}_{tr} = \mathrm{p}_2^T\hat{\theta}_{spr} \tag{20}$$

where $\mathrm{p}_2 = \begin{bmatrix} p_{12} & p_{22} & p_{32} \end{bmatrix}^{\mathrm{T}}$. The derivation of the $p_{i2}$ assumes a horizontal walking surface for the moment. In the case of non-horizontal support surfaces, the trunk-head segment pitch estimate is presumably adjusted on the basis of or replaced by visual and/or vestibular input. However, this issue is not examined here.

When $\mathrm{x}_{cb}$ is the input to the cerebellar system, $\mathrm{u}_{cb}$ is the output, and we take $\mathrm{I}_1 = 0$ (cerebellar forward integral control turns out unnecessary empirically) in Fig. 6, we can then describe cerebellar control as

$$\mathrm{u}_{cb} = \mathrm{G}_{CB}\mathrm{x}_{cb} = \mathrm{diag}(gk_i + gb_i d(\cdot)/dt)\mathrm{x}_{cb}, \quad i = 1, 2 \tag{21}$$

and

$$\begin{aligned} \mathrm{x}_{cb} &= \left(\mathrm{I} + \mathrm{I}_2\int\right)^{-1}\left(\mathrm{I}_a\int\left(\mathrm{u}_{ref} - \mathrm{P}^{\mathrm{T}}\hat{\theta}_{spr}\right) - \mathrm{F}_2\mathrm{P}^{\mathrm{T}}\hat{\theta}_{spr}\right) \\ &= L^{-1}\left\{(s\mathrm{I}+\mathrm{I}_2)^{-1}\left(\mathrm{I}_a\left(\mathrm{u}_{ref} - \mathrm{P}^{\mathrm{T}}\hat{\theta}_{spr}(s)\right) - s\mathrm{F}_2\mathrm{P}^{\mathrm{T}}\hat{\theta}_{spr}(s)\right)\right\} \end{aligned} \tag{22}$$

where $L^{-1}$ is the inverse Laplace transform, I is the identity matrix, $\mathrm{P} = \begin{bmatrix} \mathrm{p}_1 & \mathrm{p}_2 \end{bmatrix}$, $\mathrm{u}_{ref} = \begin{bmatrix} x_{com,ref} & \theta_{tr,ref} \end{bmatrix}^{\mathrm{T}}$, $gk_i$ and $gb_i$ are, respectively, proportional and derivative control gains, $\mathrm{d}(\cdot)/\mathrm{d}t$ is the differentiation operator, $\int$ is the integration operator. Thus, matrices $\mathrm{G}_k$ and $\mathrm{G}_b$ in Fig. 6 are diagonal and $\mathrm{G}_{CB}$ is a diagonal operator to represent the total processing by the cerebrocerebellar system of joint-specific proprioceptive signals. As assumed in PA-3, the cerebrocerebellar long-loop control of COM is applied to a supporting leg only. Therefore, each leg's cerebellar long-loop circuitry is turned on and off repeatedly by ground detection. This is represented by the switch in Fig. 6. No precise location of the switch is specified for present purposes. The switch implicates that cerebellar action may be scheduled according to sensory input. The cerebellar computation is described as PID signal processing based on neuroanatomical cerebellar corticonuclear modules as detailed in Jo and Massaquoi (2004). Diagonal matrix $\mathrm{I}_2$ scales integrated signal that is projected to cerebral cortex recurrently. The circuit constructs closed-loop

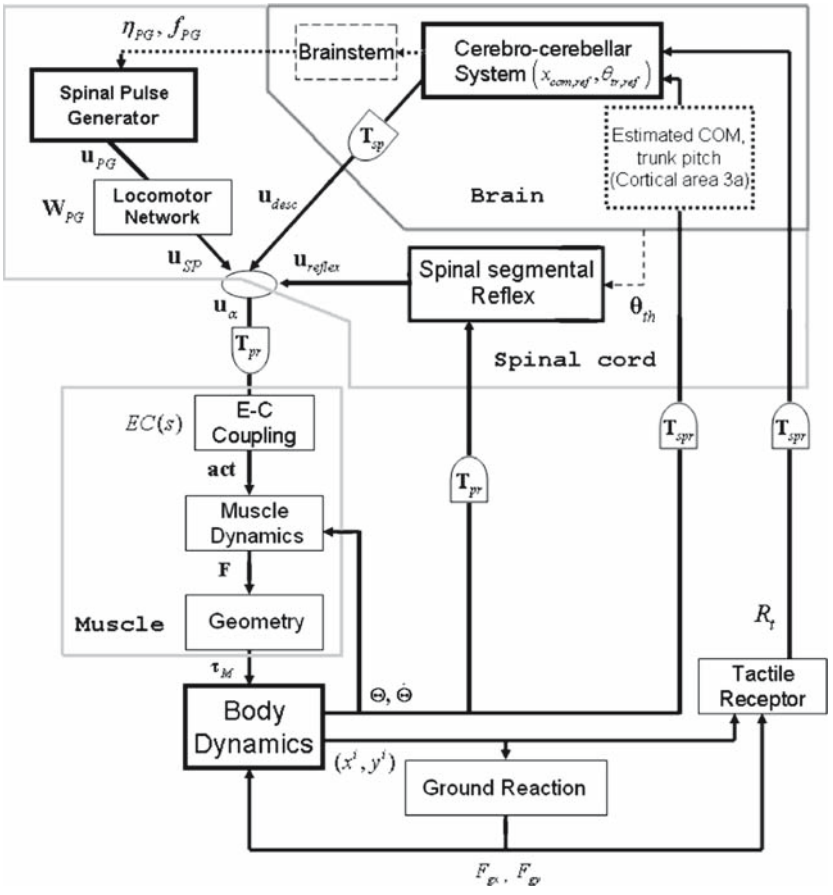


**Fig. 7** Hierarchical neural control of walking

transfer matrix $sI\,(sI + I_2)^{-1}$ that provides phase lead. $I_a$ represents scaling related to sensorimotorcortical signal integration. Diagonal matrix $F_2$ expresses the relative magnitude of the afferent signal that bypasses sensorimotorcortical integration.

Finally,

$$u_{desc} = W_C u_{cb}(t - T_{sp}) \quad (23)$$

where $W_C$ represents the distribution network in either cerebral cortical area 4 or in the spinal cord (for current purposes the location does not matter).

### *3.2.3 Summary of hierarchical neural control model*

Figure 7 summarizes the hierarchical neural control of the SBBW model. Alpha motor neuronal output $u_\alpha$ is then represented by a nine component vector. From Eqs. 17, 18 and 23,

$$u_\alpha = u_{SP}(t - T_{pr}) + u_{desc}(t - T_{pr}) + u_{reflex}(t - T_{pr}) \quad (24)$$

The cerebellum presumably plays a role in the generation of appropriate patterns of limb movements, dynamic regulation of balance, and adaptation of posture and locomotion through practice (Morton and Bastian 2004). The last function is not treated in the current model, but the first two are represented. The cerebrocerebellar system controls the COM and trunk verticality, and implicitly descends neural signals affecting the parameters in the pattern generator, which implicate a presetting or adjustment of the gain of proprioceptive reflexes and a sequence of feedforward programs. Supraspinal control including the cerebellum also can adjust the tonic excitation which coordinates the retraction of a leg. In this perspective, the cerebellar system demonstrates the first two functions.

## 3.3 Implementational assumptions and model evaluation

For tractability of the initial study, and to evaluate minimal requirements for active, moderately stable locomotion, the following implementational assumptions have been made:

– (IA-1) Movements will be driven by monoarticular muscle pairs.

– (IA-2) Spinal synergy activation will be driven by a strictly sequential train of on-off pulses.
– (IA-3) Inter-leg coordination is achieved by artificially enforced 180 degree phase difference between the pulse generators controlling each leg, rather than modeling interactive circuitry.
– (IA-4) For movement initiation from a standing start, it was assumed that a single additional pulse could be applied to hip flexors to flex the leading hip transiently.

The implications of these assumptions are considered in the discussion.

The SBBW model was then evaluated first in terms of its steady state walking features both kinematic and neuromuscular. Specifically, clinical investigators have defined the determinants of normal and pathological gait by observing features of human locomotion pattern that minimize displacement of the body's COM. This has yielded the six determinants of normal gait (Saunders et al. 1953; Della Croce et al. 2001). However, all but one — knee bending at foot impact — are not observable in the sagittal plane and therefore are not immediately useful for analysis of the SBBW model. As an alternative, the model was examined to determine whether it exhibits any of nine pathological gait features (Perry 1992). Next, the robustness of its performance was assessed by determining its ability transition to steady state walking at different speeds from a standing start, and to subsequently slow to a stop. Stability robustness was tested by subjecting the model to forward and backward impulsive disturbances during different phases of the gait cycle, and by simulating sudden additions of mass to the trunk. Finally, the sensitivity of the model behavior to several simulated neural and muscular lesions as well as control parameter variations was observed. During the simulations, all model parameters were held fixed unless explicitly stated otherwise.

## 4 Results

### 4.1 Kinematic features of walking

After an initial transient, body kinematics converged to a consistent walking pattern that was qualitatively very similar across a range of speeds. Fig. 8 shows a typical human speed of about 1.2 m/s that is simulated with $f_{PG} = 1.3$ and $\eta_{PG} = 1.2$. Initiation is discussed below and initial conditions are specified in appendix. It takes several steps to converge to steady state walking motion. The steady state motion displays a number of

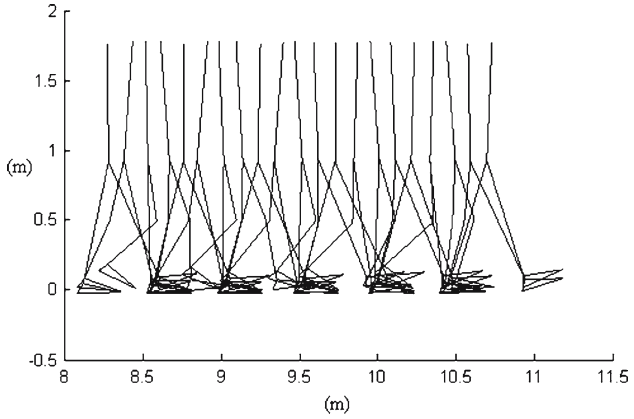


**Fig. 8** Steady state walking at 1.21 m/s sampled every 10 ms

the kinematic features (Saunders et al. 1953; Perry 1992) of natural human walking. The ankle joint trajectory (Fig. 9 *Top*) includes a valley corresponding to toe push off. In Fig. 9 d–f, this motion at the end of ground contact can also be seen as a sharp transient in coordination plots. Small bending motions at knee joint during a gait cycle correspond to impact at the transition from swing to stance, while large bending motions correspond to the retraction phase. During each cycle, the hip has a monophasic oscillation in the anterior-posterior direction. Each joint trajectory approximates a limit cycle (Fig. 9 *Top*). The ankle motion is most variable, consistent with proximity to ground contact. During simulated steady walking at 1.2 m/s with the nominal sets of parameters, each leg spends about 59% of each cycle in stance and the rest in swing. Double support phase accounts for about 9% of each cycle. These values mirror those of 60% and 10%, respectively, measured in humans (Perry 1992). The coordination of the joints is shown pairwise in Fig. 9a–c.

It has been suggested that at least 9 features can be identified in defective human gait (Perry 1992). Seven of these are observable in the sagittal plane:

1. Foot slap on the ground during loading response.
2. Flat foot contact at transition from swing to stance.
3. Knee hyperextension from loading response to midstance.
4. Inadequate knee flexion during swing.
5. Excessive forward lean of trunk during stance.
6. Backward lean of trunk during loading response.
7. Asymmetrical step length.

The third pathological feature is the complement of the third determinant of normal gait. Model steady state walking shows none of the above features (Fig. 10). The simulated motion is also qualitatively smooth.

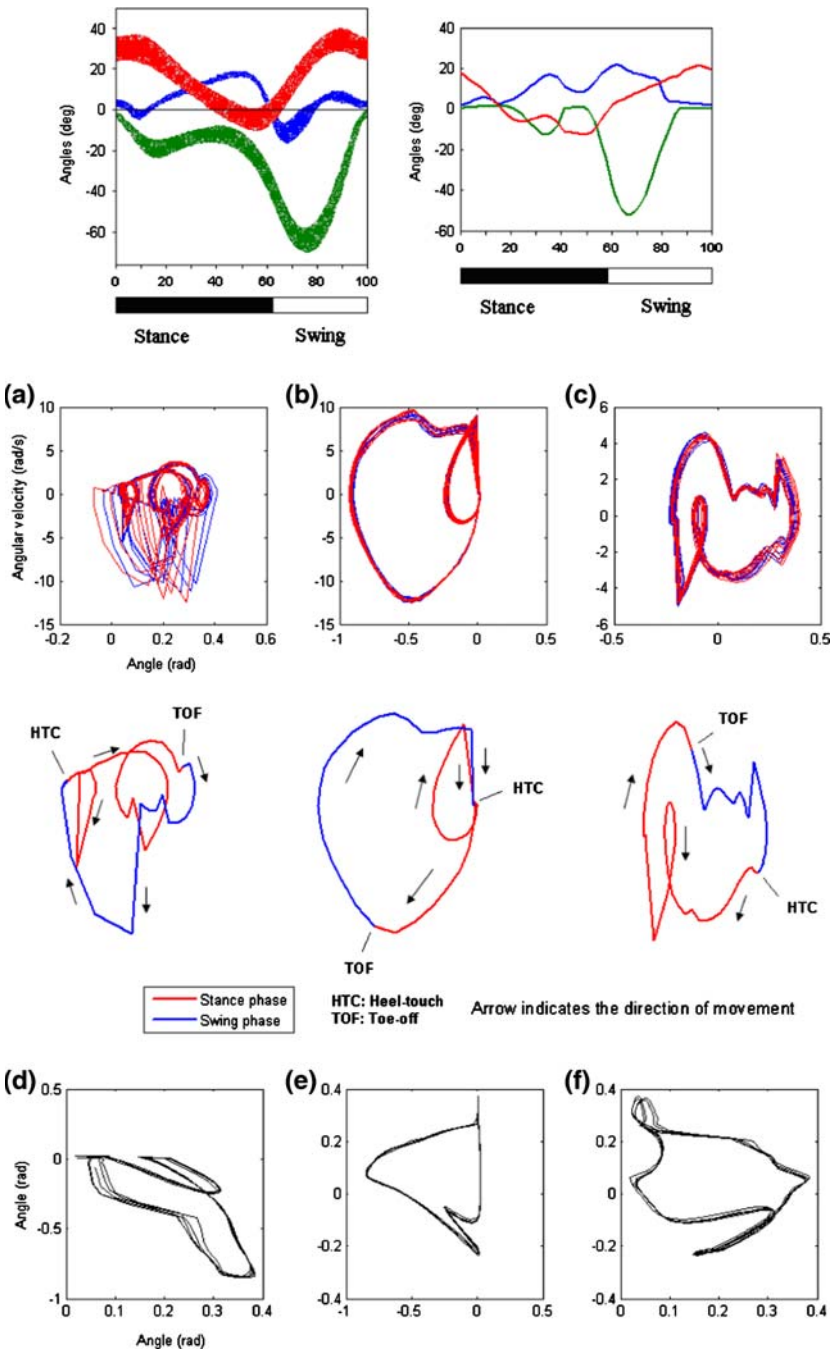


**Fig. 9** Steady state walking kinematics. *Top*: averaged time courses of hip (red), knee (green) and ankle (blue) joints during a gait cycle, (*left*): experimental data adapted from the web: CGA normative gait database (http://guardian.curtin.edu.au/cga/data/index.html), (*right*): simulation. *Middle*: joint phase-plane behavior **a** ankle, **b** knee, **c** hip (each typical cycle extracted and labeled beneath). *Bottom*: joint coordination plots: **d** ankle vs. knee, **e** knee vs. hip, **f** ankle vs. hip

### 4.2 Walking initiation

While a human maintains standing posture, the erect body tends to tilt slightly forward around ankle about 2–5° to maintain the COM within stable supporting area (see Loram et al. 2004). Therefore, an initial postural condition is set to be $\theta_a = 0.05, \theta_k = \theta_h = 0$ for both legs. Walking can be initiated from stance by applying pulses of muscular activity to IP (Fig. 11b) and then starting the NPG. The added pulse may be interpreted as a walking trigger from CNS. Fig. 11a shows that there is a transient initial response. The first step is with the right leg while the left leg supports body. Steady state walking is substantially achieved by the third gait cycle.

### 4.3 Dynamics and muscular activation

Dynamic realism is confirmed in Fig. 12 where both components of the reaction force waveform are biphasic with values of appropriate magnitude (Winter 1990).

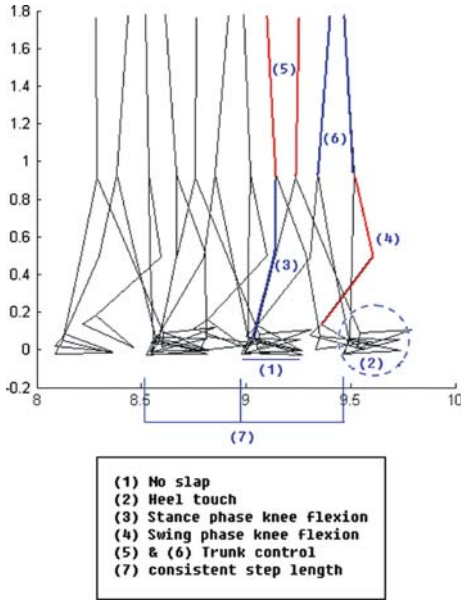


**Fig. 10** Gait analysis with respect to clinical featuers of defective gait

The horizontal reaction force is negative just after heel contact the ground, indicating a backward horizontal friction force. Then, the force becomes positive, indicating the forward reaction as the foot to pushes backward against the ground. The vertical reaction force shows a rapid rise at heel contact in excess of body weight (80 kg) to account for vertical deceleration. As the knee flexes during midstance, the force is below body weight. At push-off, a second peak greater than body weight is caused by plantarflexors. The second peak in simulation is greater than the first, which is not physiologically typical. This is due to force at the heel that is not fully realistic as will be discussed.

The patterns of muscular activation during steady state walking are shown in Fig. 13. Examining first the physiological data from Ivanenko et al. (2004, 2006), activations of GM and VA occur the LOA control epoch. Activity of SO occurs most strongly during the THR epoch, while that of IP occurs during RET, just before or during the onset of forward leg swing. BFS and TA operate during retraction and forward swing to prevent the swinging foot from touching the ground.

The activities of GM, BFS and SO are best predicted by the model. Except for minor phase shifts the waveforms are quite similar in simulation and data. IP is also fairly similar. However in the ventral muscles, the model predicts unrealistically additional activation roughly during the REG control epoch. In experimental data, there is little muscular activity during this period in any muscle. GM, BFS, SO and IP are monoarticular muscles and appear to be responsible for the bulk of the basic leg motion during walking and apparently account for much of the functional realism of the SBBW model. Biarticular muscles BFL and VA responsible for flexing and extending the knee (not shown), and uniarticular muscle TA which is responsible for lifting the foot to provide ground clearance, are least well predicted. The former are redundant from a control perspective and therefore may be inherently less predictable. The TA in vivo appears to stay active during the FOW control epoch while in simulation this was not necessary to afford ground clearance.

Principal component analysis (PCA) was applied to simulated muscle commands act. Four principal components (PC1 – PC4, Fig. 14) captured over 98% (52.2, 36, 5.6, 5.1%, respectively) of the variance in the signals. These components resemble major factor waveforms derived from published muscle activity data during human walking (Ivanenko et al. 2004; Davis and Vaughan 1993; Olree and Vaughan 1995). PC1 is comparable with FACTOR 1 in Ivanenko et al. 2004, and PC2 with FACTOR 2, PC3 with FACTOR 3, and PC4 with a combination of FACTOR 1 and 5 and negative FACTOR 4. Olree and Vaughan (1995) also retained four major factors and one of them included a combination of FACTOR 4 and 5. According to Olree and Vaughan (1995), it was inferred that FACTOR 1 presents propulsion, and FACTOR 2 loading or weight acceptance, and suggested that FACTOR 1 and 3 were in fact the same as FACTORS 2 and 4, phase shifted by 50% of a step cycle so that there are only three basic factors. They referred to FACTOR 5 as the coordinating factor because it maintained the phase shift between the left and right sides. Temporarily, FACTOR 4 corresponds to retraction of the leg. Presumably, this closely predicts the timing of loading of the opposite leg and thus may be involved in inter-limb coordination. These results indicate that despite the SBBW model's somewhat unrealistic activity during the REG control epoch, it captures overall EMG activity fairly well. It is then also interesting that some of Ivanenko's subjects displayed EMG activity in REG (red and blue traces in FACTOR 2, Fig. 14, column (b)).

### 4.4 Control of walking speed

Several parameters affect walking speed. Increase in the frequency $f_{PG}$ and magnitude $\eta_{PG}$ of spinal pattern generator signal causes faster walking (Figs. 7, 15). Control during the REG and THR epochs is responsible. Selective enhancement of IP, VA and TA, via muscle activation components IP-1, VA-1 and TA-1 (Fig. 4) during REG was found to be particularly potent (not shown).

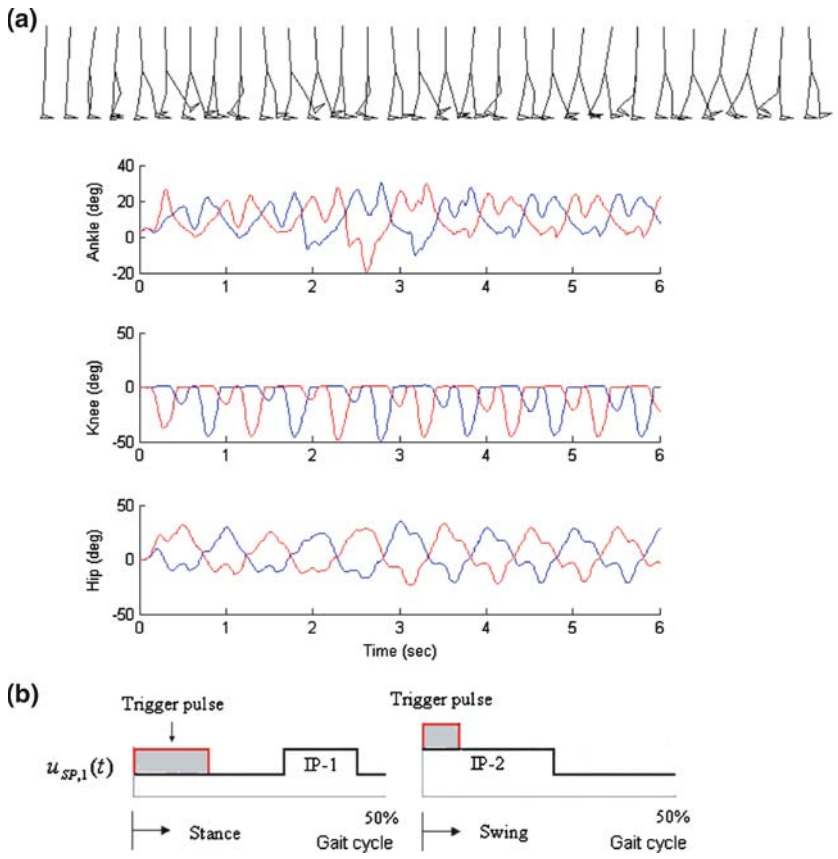


**Fig. 11** **a** Stick figure plot and joint trajectories of simulated walking initiation from stance. In the stick figure plot the motion is sampled every 100 ms and separated horizontally for clarity. Red lines indicate joint trajectories of initial swing leg, and blue stance. **b** Neural pattern for initiation: Trigger pulses are added to $u_{SP,1}(t)$ of both legs in Fig. 4 in order to initiate walking at only first step

These help move the COM forward during stance. Speed can also be increased within narrower limits by augmenting GC and SO action during the thrust epoch (component SO-1 in Fig. 4). However, this eventually has the undesirable effect of lifting the body off of the ground. The SBBW model is not equipped to tolerate this occurrence. Presumably, however, this effect could be useful in the control of running.

Appropriately, speed is also partially controllable using the reference signal $x_{com,ref}$. Increasing $x_{com,ref}$ causes the body to accelerate forward slightly during the REG epoch. For example, $x_{com,ref} = 0.18$ with $f_{PG} = 0.8$, and $\eta_{PG} = 0.9$ generates steady state walking speed of 0.65 m/s, while $x_{com,ref} = 0.25$ with the same $f_{PG}$ and $\eta_{PG}$ yields a speed of 0.72 m/s. The acceptability of increasing $x_{com,ref}$ alone is limited, however. Unless $f_{PG}$ and $\eta_{PG}$ are changed concordantly, the model eventually falls forward.

### 4.5 Stability to push disturbances and mass increase

The application of 200 ms duration forward and backward force impulses to the center of mass of the trunk-head segment were simulated at 0, 25, 50, and 75% of the gait cycle. At each gait cycle fraction, the maximal force levels from which the model could recover steady state walking were determined. Figure 16a,b shows the effects of a 70 N maximal forward impulse applied at 0% phase (toe-off) and a 75 N maximal backward push applied at 50% phase (mid-stance). Figure 16a demonstrates forward pushes cause more distance, and backward pushes less distance to be traveled within a given time. Figure 16b indicates that such a push disturbs primarily ankle motion (of the stance leg) transiently. The model tolerates forward disturbances slightly better than backward disturbances except at mid-stance when resistance to backward pushes is slightly better (Fig. 16c). After an initial deviation, the COM motion pattern is recovered within 3 or 4 gait cycles modulo a fixed phase lag or gain (Fig. 16d) that demonstrates again the absence of absolute position control shown in Fig. 16a.

The model was also tested by changing the mass of the trunk-head segment, and, therefore, also its moment of inertia, without alteration of feedforward neural commands. Thus, this change tested the inherent viscoelastic and neural feedback mechanisms. It was found that up to a 10-kg increase (18.5% of the trunk mass) could be tolerated without falling. Fig. 17b shows the effect in the phase plane. It is evident that the walking speed is lower with the increase of mass. Phase plots indicate that different limit cycles result at ankle and hip.

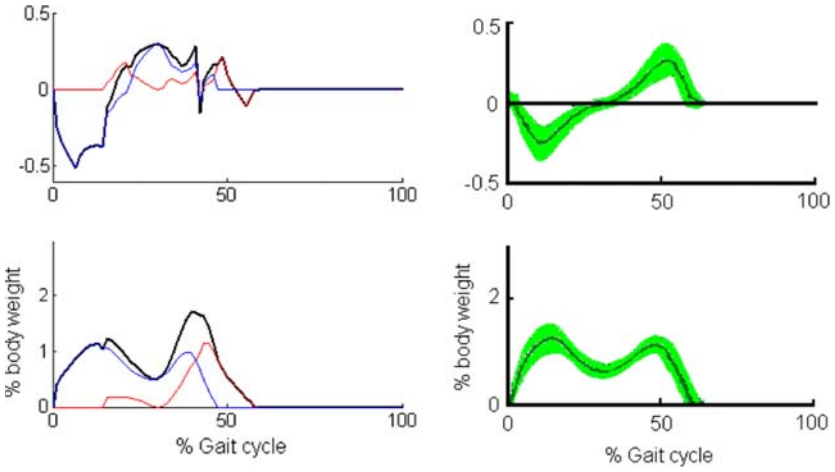


**Fig. 12** Ground reaction forces. *Left*: simulated force profiles divided by total body's weight. *Right*: typical force profiles adapted from Neptune et al. (2004). Top: horizontal reaction force profile, and Bottom: vertical reaction force profile: components of the reaction force are shown: black indicates the total force, blue force at the heel, and red force at the toe

### 4.6 Sensitivity analysis and simulated system lesions

Sensitivity analysis of the model parameters associated with the cerebrocerebellar system helps clarify their roles in walking simulation. Several gait cycles were simulated with either a 30% increase and decrease in the value of different parameters relative to their values used for nominal walking simulation (Fig. 8). Stable walking is characterized by a reproducible limit cycle as in Fig. 9. In Fig. 18, it is observed that stability is lost when there is (a) an increase of cerebellar gains ( $gk_1$ or $gk_2$), or of the gain of direct long-loop pathway to cerebellum ($F_2$), (b) a decrease of the recurrent integrator gain ($I_2$) or of $gk_2$. The model loses stability gradually with a decrease of $gk_2$. Otherwise, walking is stable. Walking is least sensitive to variation in $I_2$ indicating that the less direct long feedback loop is less important for walking that it is for balance (see Jo and Massaquoi 2004). $gk_1$, the proportional feedback control gain of the COM, is not as immediately critical for stability in walking as is $gk_2$, the proportional feedback control gain of the trunk pitch. Increased gain values at the moment have no obvious clinical counterpart, but indicate that there are practical limits to the feedback loop strength. Decreased $gk_i$ would correspond to loss of either deep cerebellar nuclei or mossy/parallel fibers that is generally associated with clinical ataxia. Reduced $I_2$ is consistent with interruption of cerebellar outflow signals as occurs commonly in multiple sclerosis where it produces a violent tremor (Massaquoi and Hallett 2002). Inappropriate selection of $F_2$ would correspond to malfunction in either spinal or supraspinal sensory nerve. Sensitivity to the parameters proposes a rudimentary idea about behaviors of neural lesions. Simulations with inappropriate parameter values presumably consistent with neurophysiological malfunctions are demonstrated in Fig. 19. These do not analyze lesions rigorously, but propose simple insights into the SBBW model with respect to biological plausibility.

Figure 19 shows the effects of removing trans-cerebellar long-loop control of COM and trunk pitch, weakening the recurrent integrator and eliminating the peripheral modulation of synergies. In Figs. 19a–c, the body fails to maintain a sufficient step size causing forward tripping. Figure 19d demonstrates that swing leg retraction is not fully achieved due to inappropriate large knee excursion so that toe eventually scratches the ground. That causes the forward trip again. In the model, the simulated lesions in the trans-cerebellar long-loop control give rise to forward tripping due to a failure of balance control of supporting leg while the lesion of the presynaptic inhibition disturbs swing leg excursion. To test pathological walking behaviors in even further detail, cerebellar long-loop control of the swing leg should be modeled along with a possible role of the cerebellum in scaling feedforward NPG signals.

## 5 Discussion

The SBBW model attempts to account for the primary kinematic, dynamic and physiological features of human locomotor control with a formulation that is simple in structure and control principles. This approach is motivated by the assumption that nature may often prefer simple, robust solutions to motor control problems. The work continues along the lines of Taga (1995) and Ogihara and Yamazaki (2001), and provides more detail regarding possible neural control mechanisms and more extensive evaluation of the stability and performance characteristics that result. Specifically, it is demonstrated

that when balance is stabilized by two specific long-loop stretch responses, stable walking with many realistic features can be afforded by a five sequential-state spinal pulse generator that distributes pulse-like activation to muscles organized in four control synergies. Model walking demonstrates natural convergence to a consistent steady-state gait pattern over a fair range of speeds and simultaneously displays significant resistance to pushes and weight changes. Walking speed can be increased by a monotonic increase in central pulse generator intensity and frequency without other control modifications. The simulated muscle activation patterns share important similarities to experimental observations, but also show differences that remain to be reconciled. Successful walking is demonstrated to depend on the intactness of most components of the control system suggesting that the model is of fairly minimal complexity. Importantly, there is no apparent requirement for internal models of body dynamics, detailed programming of joint motions or explicit computation of torque demand at any joint. Also, it appears that muscle synergies, together with composite signal feedback, can enable multi-joint feedback control to be implemented by simple Single-Input Single-Output (SISO) modules. The proposed control mechanism is argued to be broadly consistent with cerebrocerebellar and spinal/brainstem systems.

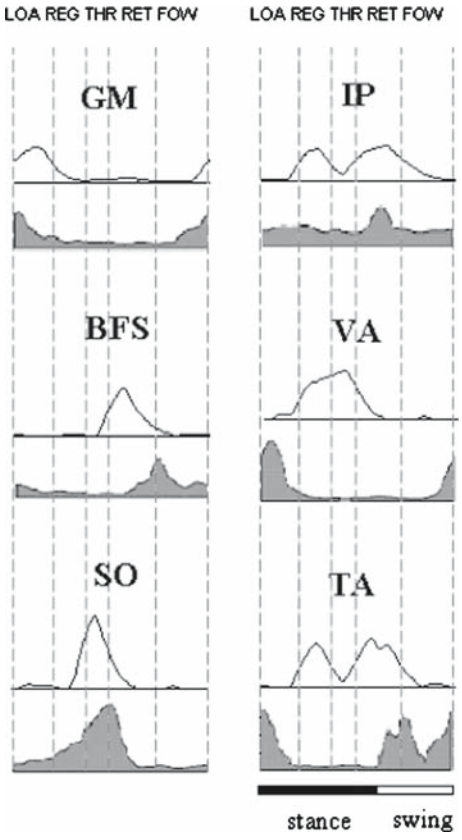


**Fig. 13** Simulated (upper trace) and observed EMG patterns (*bottom filled gray*) during a gait cycle arranged anatomically. Data is adapted from Ivanenko et al. (2006)

### 5.1 Kinematic qualities of simulated gait

The SBBW model accounts for a number of kinematic features of natural walking without requiring detailed programming of joint time-courses. The feedforward control signals consist of a steady intended forward displacement of the center of mass, a vertical reference for the trunk angle and a series of non-overlapping rectangular spinal neural pattern generator signals to cause stepping. Apparently, the long-loop and segmental neural feedback, muscular synergies, muscle viscoelasticity and activation dynamics are sufficient to add the coordination and modulation necessary to produce smooth, stable, natural appearing movements. The convergence to a consistent steady state cadence is not surprising given the regularity of the NPG. However, this was not a necessary outcome. The system dynamics include instability and many significant nonlinearities and ground contact is intermittent. Therefore, the gait could become unsteady, as is the case when there is reduced control at joints (Fig. 19).

Body kinematics are well summarized by joint angle, joint coordination, phase-plane and single/double support fraction data. Joint angle data shows slightly less knee flexion and ankle plantarflexion during the RET and FOW control epochs than seen in experimental data. This may relate to the model's failture to reproduce hip drop in the swing leg, as discussed below. However, the kinematic analysis indicates that body motion is generally quite realistic. Consistent with this, it was found (but not shown here) that the kinematics lie naturally close to a plane in three dimensional joint-space. This feature has been identified in human subjects (Lacquaniti et al. 1999) in terms of *elevation angles*, the angles between body segments and a vertical reference. The transformation between joint angles as used in this study, and elevation angles is affine. Therefore planarity in either system implies planarity in the other. Functionally, planarity corresponds to the fact that although the four segments defining body and leg configuration have in principle four degrees of freedom, during walking they exhibit two. The trunk is constrained to be always nearly vertical and the legs function primarily as swinging pistons that exhibit rotation of the leg at the hip and flexion and extension of the leg. For the most part, the upper and lower leg and foot move in unison. That the trajectory is substantially a single closed loop indicates that the two underlying degrees of freedom

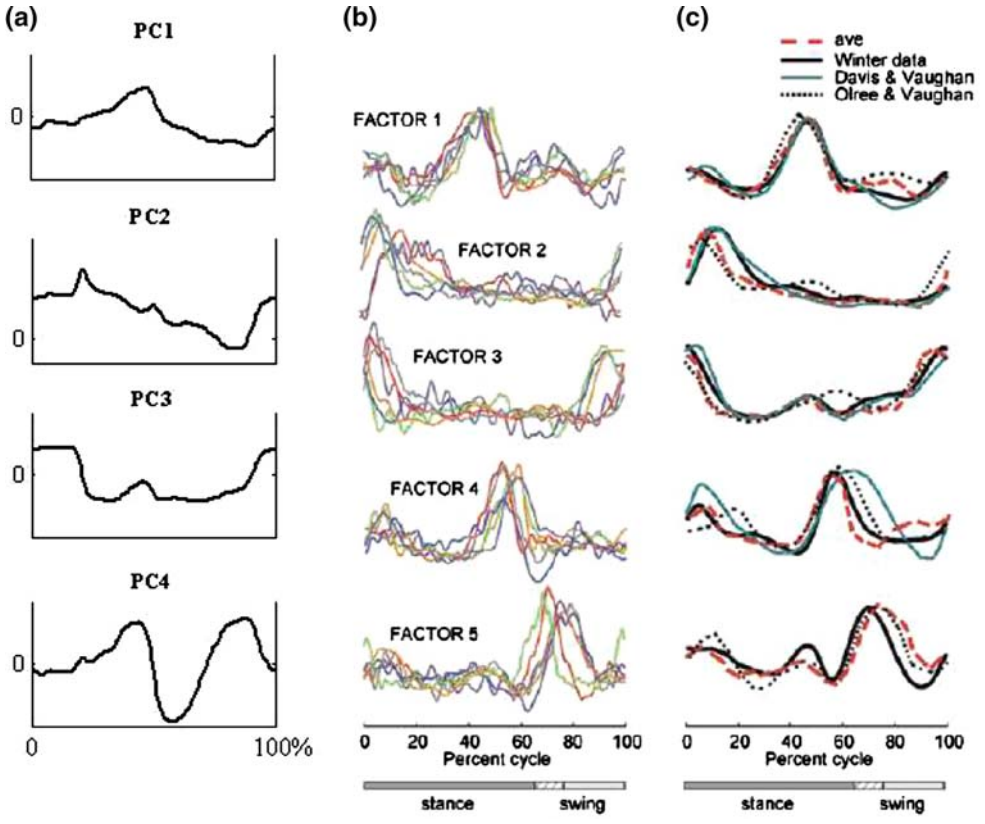


**Fig. 14** **a** Principal components of simulated EMG patterns in a gait cycle. **b** and **c** Factors summarized from human EMG data: **b** Several individual subjects from Ivanenko et al. (2004). **c** Comparison of principal factors from other studies (Winter 1991; Davis and Vaughan 1993; Olree and Vaughan 1995) adapted from Ivanenko et al. (2004)

are coordinated in a consistent manner at the same frequency. The principal partial exception to this analysis is that the ankle motion during ground contact is slightly more complicated. During early stance phase, $\theta_1$ (or $\theta_2$) increases somewhat while $\theta_3$ (or $\theta_4$) declines slightly as the stance leg straightened. This is opposite to the overall coordination pattern between knee and ankle and results in a transient deviation from the plane. This can be seen in human data as well (Lacquaniti et al. 1999). Planarity is recovered quickly with the rapid ankle plantar flexion flick at the end of ground contact. On average, the behavior remains that of a swinging piston.

As the SBBW model addresses only sagittal plane performance and approximates the action of muscle groups without including, for example, variations in moment arm with joint angle, full Hill-type muscle dynamics (Winters and Stark 1985; Zajac 1989) and the action of toes. Therefore, no attempt was made to match the kinematics of a particular human subject precisely. Nonetheless, the most characteristic aspects of natural walking appear to have been captured. This is also true in terms of clinically-oriented walking assessment scales.

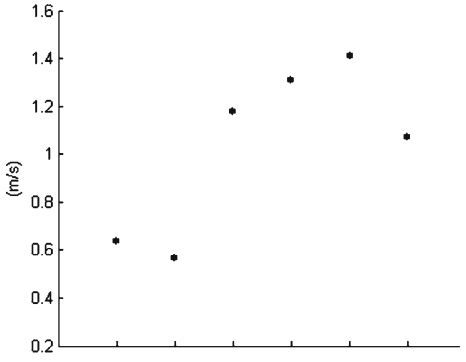


| $f_{PG}$ | 0.8 | 0.9 | 1.0 | 1.1 | 1.2 | 1.3 |
|---|---|---|---|---|---|---|
| $\eta_{PG}$ | 0.9 | 1.0 | 1.12 | 1.15 | 1.17 | 1.2 |

**Fig. 15** Steady state walking speeds afforded by changing frequency $f_{PG}$ and magnitude $\eta_{PG}$ of spinal pulse generator

## 5.2 Feedforward command signals

The major features of gait kinematics were produced by the empirically-developed feedforward action of a spinal pulse generator and four muscle control

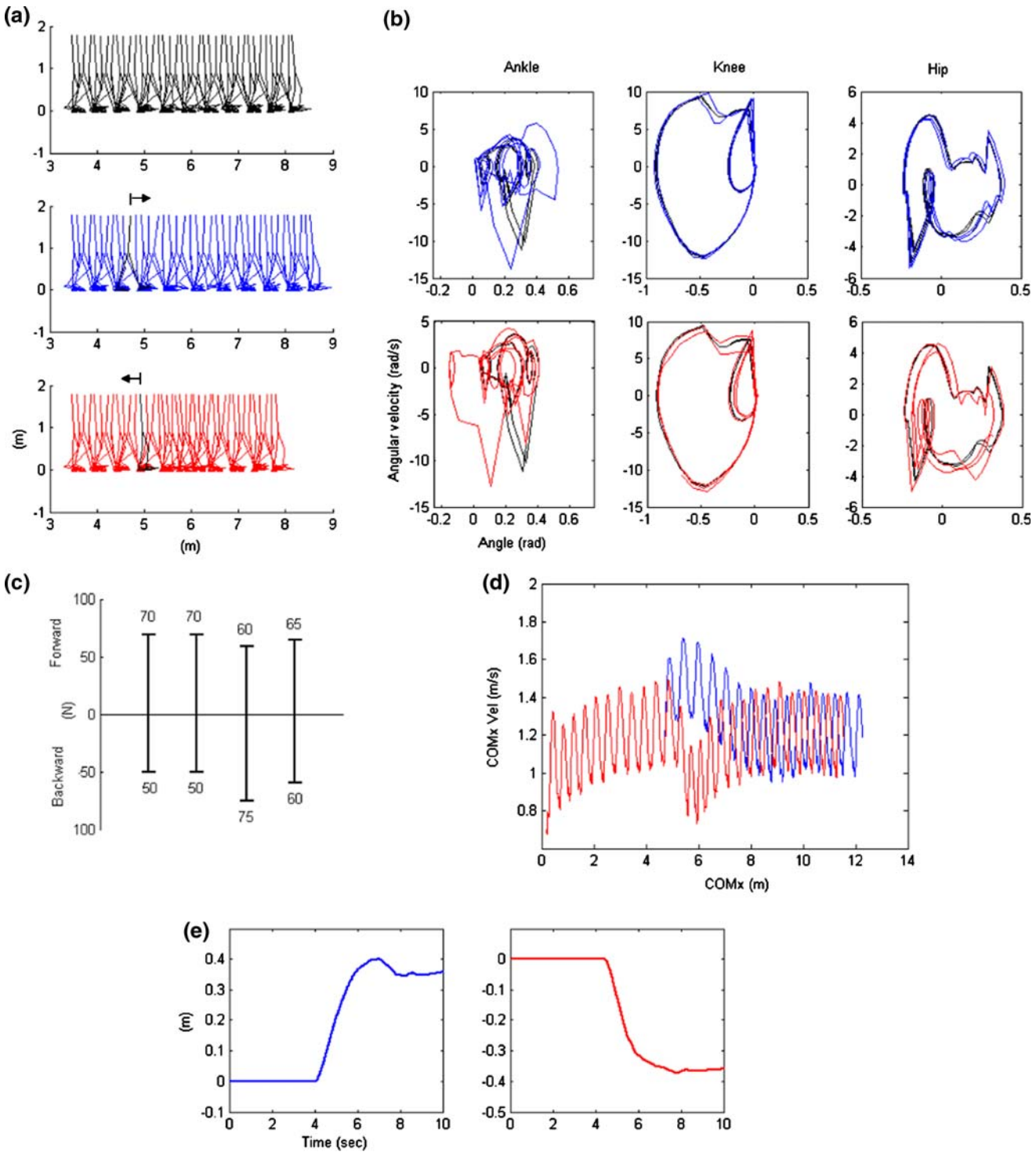


**Fig. 16** (Simulations of disturbed and normal walking. (**a** *top, black*) undisturbed; (**a** *middle, blue*) walking pushed forward by 70 N at 0% phase, (a: *bottom*, red) walking pushed backward by 75 N at 50% phase; the black stick figures under arrows indicate the timing of the impulse applications in duration of 20 ms. **b** Corresponding phase plane plots of ankle, knee, and hip (left leg only) to compare disturbed and normal walking. **c** Maximal forces tolerated in each phase. **d** Phase plane plot for COM with disturbed walking: Response to 70 N forward impulse at 0% phase (*blue*), 75 N backward impulse at 50% phase (*red*). **e** Trajectory of horizontal COM (COMx) deviation between disturbed and normal walking, (*left*) walking pushed forward by 70 N pulse at 0% phase — normal walking, and (*right*) walking pushed backward by 75 N at 50% phase — normal walking

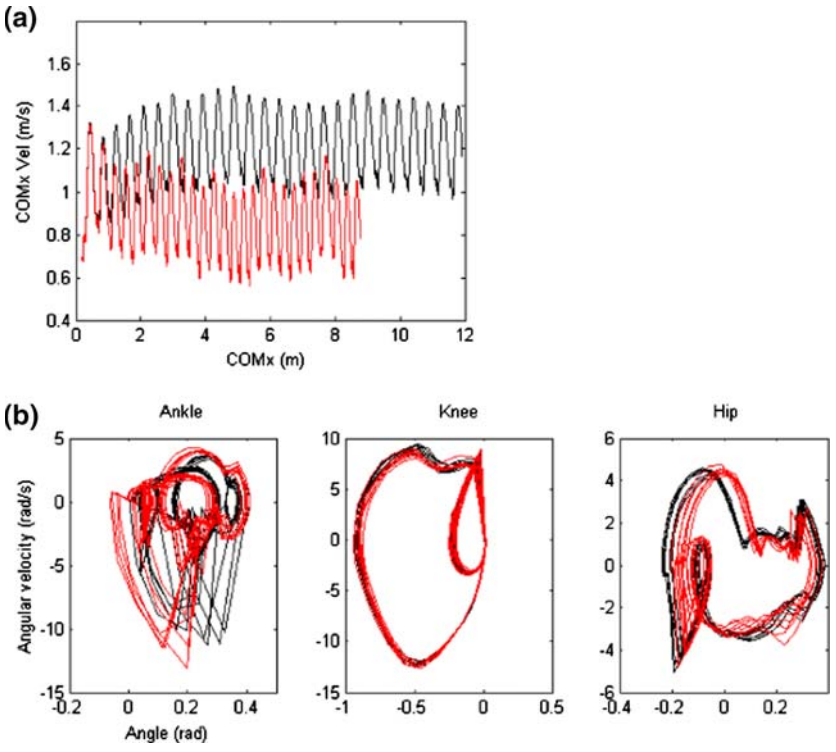


**Fig. 17** **a** COM patterns (forward COM position vs its velocity), **b** phase plots of ankle, knee, and hip from left to right (left leg only); nominal walking pattern (black), increased trunk mass (red)

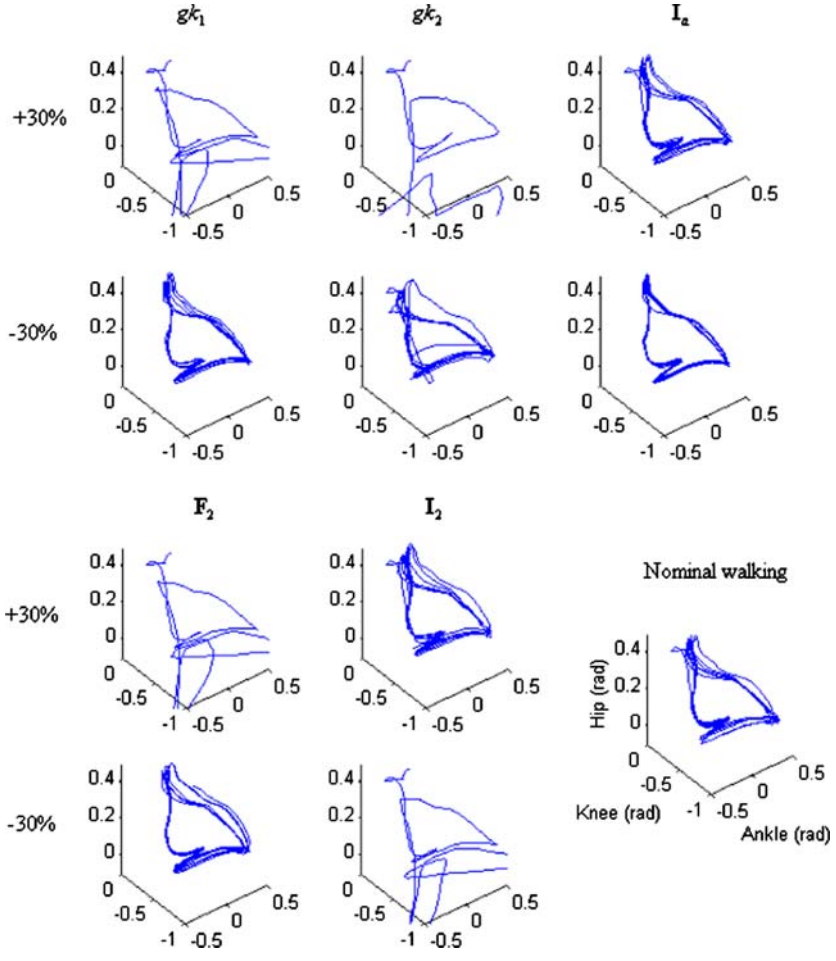


**Fig. 18** Sensitivity to neural parameters. Simulated motions with each parameter increased by 30% and decreased by 30% are drawn and compared with nominal walking motion with no change of parameters

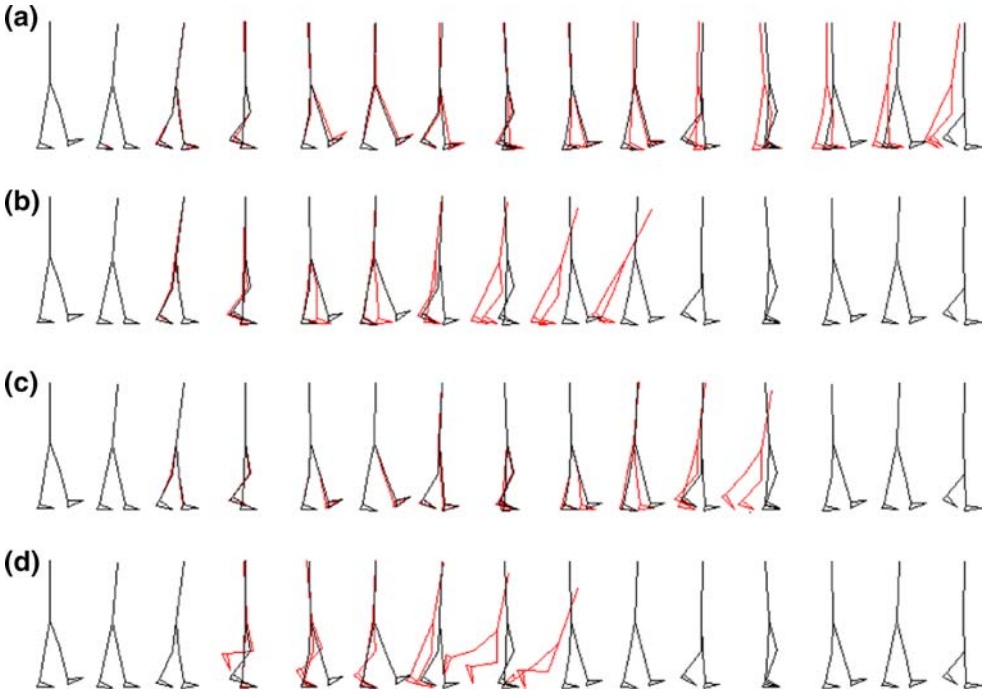


**Fig. 19** Stick plots (red) of **a** no trans-cerebellar long-loop control of COM, **b** weakened trans-cerebellar long-loop control of trunk pitch, and **c** weakened recurrent integrator; **d** eliminated segmental reflex in comparison with normal walking (black). Each motion is sampled every 100 ms, but is horizontally relocated for clarity. *Thick blue line* indicates the ankle trajectory, the *dotted green* the knee, and the *thin red* the hip

synergies that it drives. A steady (tonic) reference command that specified a forward displaced COM enhanced walking speed as discussed below, but actually was not required for walking as long as COM and trunk pitch were under feedback control. Other central neural pattern generator schemes have used separate pattern generators assigned to each joint to define independent and continuously varying intended trajectories. The SBBW model uses a simpler approach. Differently scaled but similarly shaped pulses delivered during five sequential control epochs: Loading, Regulation, Thrust, Retraction, and Forward swing, were found to be the minimal arrangement that could account for a full range of walking speeds by scaling epoch durations proportionately. This resulted in the constancy of EMG pattern across speeds that has been noted experimentally (Ivanenko et al. 2004). This is also consistent with the suggestion that the CNS may generate only a few basic patterns of muscular activity for locomotion (Patla et al. 1985). The pulse generator command was selected to consist of rectangular pulses for simplicity. In fact, because of the significant low-pass filtering characteristics of muscle activation and impedance, net locomotor behavior is not especially sensitive to high-frequency details of muscle command signal morphology. Any type of pulse-like waveform (see also Cajigas-González 2003) can have substantially similar effect. Thus, the spinal level is considered to implement equilibrium trajectory type control (Fledman 1986; Bizzi et al. 1992), the performance of which is enhanced by more realistic activation level-dependent muscular viscoelasticity.

Initiation of movement required a small additional trigger pulse applied to hip flexors during the first step. This component essentially provides the initial swing leg elevation and forward momentum that would ordinarily be contributed by substantially passive dynamics in the middle of the gait cycle. That participation of a separate system, such as the basal ganglia, may be required to begin walking is a conjecture. However, it is consistent with the particular deficit in Parkinson's Disease wherein the initiation of walking may be disturbed preferentially. However, more analysis will be required to characterize such a system.

### 5.3 Dynamics and muscle activation

During double support, a biped is a closed kinematic linkage (Pandy and Berme 1988). As such, there exists no unique solution for the torques at each joint. Moreover, in general, correct kinematics implies only correct net torques. Given the agonist-antagonist organization

of the muscles and the redundancy of actuation, the forces applied by individual muscle groups are not determined by the body motion. Therefore, it was important to verify that model forces and muscle activations are realistic. This can be done explicitly for ground contact for which there is considerable experimental data. The biphasic force profile with larger forces at heelstrike and toe-off is consistent with significant control at the ankle rather than the hip. This is quite realistic. The somewhat greater toe-off pulse in the simulation appears to result from the inability to reproduce in simulation the full stiffness of a typical floor. As a result, there is a mild bounce forward from rear foot to forefoot.

For approximation of joint torques, where less experimentally measured force data is available, the EMG pattern can serve as a crude surrogate if it is assumed, as is here, that the muscle model is reasonably accurate under the conditions studied. Overall, the control system appeared to generate muscle activations that were similar to those observed *in vivo*. In particular, the finding of four principal independent waveforms in muscle activation corresponds closely with the four or five factors that have been found in human data. These appear to correspond approximately to the five principal control epochs that have been proposed here. During each epoch, the muscle activation pattern tends to be quite different from the others which yields their independence, and near orthogonality. The epoch-specificity of the EMG is related to the significant differences in locomotor task during each period. Accordingly, analysis of phase-specific locomotor requirements may shed some light on the two features of predicted EMG that were potentially least realistic. These were: (a) the inappropriately predicted more widespread inappropriately predicted muscular activity during the REG control epoch and (b) the model's failure to predict TA activation throughout swing.

As pointed out above, EMG records from humans occasionally show activity during the REG control epoch. However, others clearly do not. Two effects may be important. Activation of VA and RF during REG was found to be important to keep the knee from buckling during stance. In principle, however, this is not a problem if the knee joint is substantially vertical or even locked in extension. This stabilizing requirement is very sensitive to small changes in knee angle. It is therefore quite possible that a model with more realistic muscle viscoelastic properties, and/or enhanced segmental or long-loop reflex action during LOA could obviate or reduce muscular action during REG.

In addition, during REG and THR that the ankle has its greatest efficacy in body control, especially during slow walking. This is because it is during late REG and early THR that the COM lies above the base of support. During LOA the landing leg is extended forward. Because of the geometry of foot placement, muscular dorsiflexion at the ankle during LOA acts to stiffen heel contact and can thereby contribute to COM deceleration. But active plantar flexion can contribute little to forward COM acceleration. Conversely, late in THR, the COM is forward, beyond the foot. Active plantar flexion can contribute significantly to accelerating the COM forward (and up). But dorsiflexion has little effect on COM deceleration. During late REG and early THR (midstance), however, the ankle can accelerate or decelerate the body. In particular, to accelerate the body, the ventral muscles, IP and VA, are activated as well as TA, as shown in Fig. 4. Importantly, throughout stance phase, the thigh adductors, especially the adductor magnus (well developed in sprinters), can contribute to hip extension and thus to COM acceleration. These have the advantage over not lifting the body. These muscles are often not recorded experimentally, and were not included in the current simulations.

The failure of the SBBW model to anticipate prolonged activation of TA may relate to the fact that the model only describes motions within the midline sagittal plane. Natural walking includes a small amount (about 6 degrees) of shifting pelvic tilt in the frontal plane that results in about 5 cm of drop of the swing leg hip (Inman et al. 1981). While subtle, this potentially interferes with foot ground clearance. Extended activation of the TA *in vivo* may be required to compensate for this tilt. Thus, the absence of direct swing leg control during the FOW epoch may account for the finding of four rather than five principal components in the muscle activation signals. Arguably, the 'missing synergy' includes activity of BFS, BFL and TA during swing that helps to maintain the leg in retraction. This would presumably correspond to the fifth FACTOR identified in experimental EMG data. In any case, it appears that EMG control during early to mid-stance and early to mid swing in the opposite leg is likely to be important, and sensitive to many factors. This suggests that more data will be required to determine the variety of possible muscle activation patterns that can be effective.

### 5.4 Stability

Steady state walking with limit-cycle characteristics was shown to follow from a standing start using only a step change in forward commands and a launching pulse applied to IP. This is not necessarily a realistic command process but was employed to underscore the model's inherent stability and to emphasize potential simplicity

of forward control. Steady walking resisted modest impulsive disturbances and mass increases without changes in parameters or changes in feedforward control signals. These alterations stressed the limit cycle-like behavior described above and suggest that the stabilizing characteristics of the mechanics and control scheme are fundamentally sound. The SBBW model's feedback control system is particularly simple and corresponds well with the two channel control of posture posited on the basis of human studies (Freitas et al. 2006). To some extent, this is quite expected based on first principles. Minimal necessary conditions for upright walking are (a) maintenance of the COM near the base of support, and (b) maintenance of trunk verticality. During single leg support, this means that the COM should be roughly over the foot, and during double support phase, the COM should be roughly within the convex hull of the two feet. These conditions are evidently fairly easy to achieve using long-loop feedback, especially when control is applied grossly to whole limbs. This is facilitated by the use of multiarticular synergies. As discussed further below, this approach has potentially important implications for cerebellar functional architecture and to our knowledge has not been used previously in simulations of natural locomotion or in robot locomotion control.

Limited exploration of the sensitivity of walking to simulated system lesions indicates that it is likely that all system components must be reasonably intact for successful walking. This suggests that the model has a generally parsimonious structure. In principle, there are a limited number of failure modes. The COM can fall forward, backward or directly downward. For the latter to occur, the knees must buckle. Given adequate activation of the knee extensors VA and RF, or extension of the knee by other means during the REG epoch, this is unlikely. If the body falls forward or backward, either the legs spread in a "split", or the swing leg encounters the ground causing a trip. In all simulated system lesions, the body tripped forward. This is most likely when there is appreciable forward momentum and typical in cerebellar disease and severe sensory neuropathy when vision is removed. A propensity to trip is seen in toddlers and indicates that strong management of toe clearance is critical to improved locomotor control. This presumably would be the primary responsibility of activations of BFS, BFL and TA during swing.

### 5.5 Limitations in performance and stability

The model displays the ability to begin walking from a standstill, and some capacity to adjust its walking speed in response to simple changes in the feedforward commands. However, control of deceleration and walking speed was limited. In particular, slowing and stopping to a standing balance was not achieved by the SBBW model. Slow walking requires prolonged time in single leg stance phase. This places particular demand on the balance system. While it is expected that a more complete balance mechanism such as that possessed by the FRIPID model (Jo and Massaquoi 2004) would be stable under these conditions, the more rudimentary SBBW model has difficulty. This finding seems grossly consistent with the difficulties that toddlers often have in stopping without falling down. Quickly slowing to a stand apparently requires more precise control to cancel forward linear and angular momentum simultaneously using the legs, and/or strong standing balance mechanisms to dissipate residual energy without moving the feet. Thus, it appears that some type of smooth 'clutch' is needed to properly coordinate the walking and standing balance systems during slow walking and stopping. As suggested above, another important factor is likely to be control of the swing leg. This could include long-loop feedback as well as feedforward spinal input. Moreover, the current model balances upright only with enhanced ankle stiffness. While this level of stiffness is within physiological range, more complete feedback as used in the FRIPID balance model has the potential to afford superior balance control with more modest ankle stiffness.

### 5.6 Implications for neural architecture

It has been shown experimentally that electrical stimulation of the posterior structures of the lumbar spinal cord can induce patterned, locomotor-like activity (Dimitrijevic et al. 1998). Importantly, focal stimulation elicits synchronous rhythmic EMG activities in muscles at different joints in the lower limb. This suggests that neural oscillators are not joint specific and is highly consistent with the synergies used here. A synergy is a fixed relationship of activities within a set of muscles that may be modulated and/or time-shifted as a whole, but is otherwise kept intact. Synergies have generally been defined in terms of EMG, both time-dependent and time-independent formulations (d'Avella and Bizzi 2005; Cheung et al. 2005), and in terms of function (Cajigas-González 2003). These views are compatible with different emphases. The latter could be shown to account for the swinging piston-like behavior of a frog's leg during walking, swimming and wiping behaviors. In fact, a significant range of frog leg behaviors could be accounted for by the four kinematic control synergies. Similarly with the kinematic control synergies, the driving temporal waveforms in the SBBW model are taken to be simple pulses that have scalable intensity

and duration. While a rich variety of time-varying activations can be afforded, the control is ultimately constrained significantly by these assumptions. In any case, the SBBW model supports the possibility of time-invariant control synergies mediated by effectively fixed, linear connections between spinal pulse generator circuitry and motor neuron pools, thereby decoupling and simplifying the temporal and distributional components of limb control.

Recent work in the frog indicates that as previously suspected, peripheral sensory feedback may modulate the expression of motor synergies (Cheung et al. 2005). However, in general, this is found to be relatively minor effect in that basic leg behaviors are retained following peripheral deafferentation. On the other hand, upright bipedal locomotion places particularly strong demands on the control of leg trajectory. The SBBW model finds it extremely useful to have some modulation of especially the retraction control phase according to sensed leg position. Presynaptic inhibition in spinal cord as assumed by the model has been identified (Rudomin and Schmidt 1999; Baxendale and Ferrell 1981; Duysens et al. 2000; Rossignol et al. 2006). Absence of this mechanism results in simulated walking with excessive leg retraction reminiscent of the high-stepping gait of *tabes dorsalis*, a syphilitic condition involving compromised sensory input to the spinal cord (Ropper and Brown 2005). This suggests the basic plausibility of the mechanism. However, more extensive analysis will be required for validation.

While many studies show the existence of muscle synergy organization at the spinal cord level, and spinalized cats display roughly normal locomotor patterns when suspended and placed on treadmills (Lam and Pearson 2001; Hiebert and Pearson 1999; Kandel et al. 2000), it is also clear that supraspinal control is extremely important to fully normal locomotor function (Morton and Bastian 2004; Dietz 1992; Shik and Orlovsky 1976; Brooke et al. 1997; Nielsen 2003). Therefore, it was important to model supraspinal mechanisms. In particular, it was of interest to determine whether feedback control of walking could be implemented stably by transcerebellar long-loop mechanisms using low-order linear dynamics, and that control could be tuned in terms of simple linear scalings and thresholds. As argued elsewhere (Jo and Massaquoi 2004; Massaquoi 1999) the cerebellum is very likely to provide important, but simple scaling and dynamic processing for many centers within the central nervous system. While not explicitly attributed to cerebellar circuits, the scheduled scaling of especially the amplitude of NPG output with movement speed (Fig. 15) could also be implemented or at least refined by cerebellar circuits. More detailed study of control derangements in cerebellar disease will be needed to determine the validity of this conjecture.

In contrast to the FRIPID cerebrocerebellar balance control model, the SBBW model indicates that the cerebellar contribution to body control may be represented by a diagonal matrix with elements of form $(gk + gbd(\cdot)/dt)$. This is potentially an important simplification in comparison with the full $3 \times 3$ matrices of the FRIPID model (Jo and Massaquoi 2004) that represent explicit coordination of multiple joints. In the SBBW modek, cerebellar modules process signals independently while the coordination of different muscles is managed by extracerebellar synergy circuits represented by the columns of $W_C$. While the two views are not mutually exclusive, the latter is particularly compatible with recent anatomical studies (Kelly and Strick 2003) that emphasize very narrow point-to-point modular processing by cerebellum, rather than switchbroad-like fan-in and fan-out that was usually assumed. Moreover, the only gainscheduling (see Jo and Massaquoi 2004) needed by the SBBW model was that based on detection of foot-ground contact. COM and trunk pitch feedback gains were applied to signals obtained from the stance leg only.

### 5.7 Implications for robotic locomotor control

The SBBW model demonstrates that explicit computation of body dynamics is not required for control of natural walking that is robust to modest disturbances. Three features appear to be primarily responsible. First, its feedback systems provide basic upright stability via independent control of COM position and trunk pitch. Second, its feedforward pattern generator activates particular synergies each of which performs a separate dynamic function that is required within every gait cycle. Thus, in the central feedforward and feedback circuits, there is substantial decoupling of the various control circuits, while control of muscles become coupled. Both design features decrease complexity, but at the expense of reduced behavioral flexibility. The architecture allows considerable independence in neural tuning, but only of specific degrees of freedom that are relevant for bipedal locomotion. Control of the body into arbitrary configurations is not possible using this system. Presumably, body control for other behaviors must be provided by other neural components. Finally, the viscoelasticity of the muscles smoothes the effects of command inputs and enables stable contact with the ground without explicit computation of joint torques or foot forces (Hogan 1985). Many of these features are relevant for the control of artificial humanoid robots if driven by series elastic actuators (Blaya and Herr 2004) that

behave much more as muscles than do typical torque motors.

The control and mechanical properties of the SBBW model lie between those of different artificial bipedal walkers. Passive walkers (McGeer 1993) may exhibit very natural appearing gait patterns, but characteristically only for a narrow speed range that is dictated by the walker's geometry and mass distribution, and by the slope of the decline. Gently actuated, near passive walkers can traverse horizontal ground by injecting energy via foot plantarflexion (Collins and Ruina 2001) and rearward rotation at the hip (van der Linde 1999). However, because of the lack of active stabilizing feedback, these walkers also exhibit a fairly narrow speed range and also do not resist external disturbances well. At the other end of the spectrum, fully actuated humanoid robots such as ASIMO developed by Honda motor corporation (Hirai et al. 1998) demonstrate highly flexible position control of all body segments. However, in general, they are comparatively heavy, energy inefficient and have control that relies on much more complete specification of joint angle trajectory together with joint torque computation based on the relative relation between zero moment point (ZMP) (see Vukobratovic et al. 1990) and COM.

Although not investigated extensively here, the energetics of the SBBW model are likely to be favorable. First, all synergies are organized to minimize muscular coactivation. Each synergy activates only muscles that do not directly compete with each other at any joint, and each central command source drives only one synergy at a time. The current implementation uses substantially passive leg swing that likely contributes to energetic efficiency. Preliminary analysis shows that $C_{mt}$, an index used to measure mechanical energetic efficiency, is defined (Collins and Ruina 2005) as

$$C_{mt} = \frac{\text{mechanical energy used}}{(\text{weight})(\text{distance traveled})} \tag{25}$$

For the SBBW model, $C_{mt}$ is about 0.09 without any attempt to optimize this value. Passive and near passive walkers have generally shown $C_{mt}$ less than 0.1, and humans $C_{mt}$ of about 0.05, while ASIMO has a $C_{mt}$ of 1.6 (Collins and Ruina 2005). This supports the impression that SBBW model already provides a fairly realistic description of human locomotion and suggests that human-type actuation and control may afford considerable locomotor performance and stability without incurring great loss of energetic efficiency. However, further investigation including estimation of metabolic costs of muscle activation will be required for a full energetic characterization.

**Acknowledgements** The authors thank Profs. Rodney Brooks and Hugh Herr for valuable comments and an anonymous reviewer for useful suggestions. This work is partially supported by NSF KDI grant IBN-9873478 and by Fernando J Corbato fellowship and Harold E Edgerton fellowship from MIT EECS department.

## Appendix A

- Neural transmission delays
  Closed-loop transmission delays are conservatively taken to be 60, 70, and 80 ms for long-loop response to and from the hip, knee, ankle, respectively based on 50 m/s neural conduction velocity, and five synaptic delays of less than 1ms.
- Tactile receptor on the foot.
  The interaction between foot and ground is detected by tactile receptors on the foot. The signal from the receptor is expressed by $R_t$.

$$R_t = 1\left[F^t_{gy} + F^h_{gy} - \delta_F\right]_+$$

where $\delta_F$ is an offset (a small amount of force). For simplicity, detection is based on the total reaction force on the foot, which is a sum of reaction forces on the toe and heel. $R_t$ is 1 when foot receive reaction force and 0 otherwise. Therefore, the tactile receptors inform of whether each leg is at either swing or stance phase.
- Estimate of COM

$$\begin{aligned}
\hat{x}_{com} \approx\ & \frac{m_1}{(m_1+m_2+m_3)} r_1 \sin\theta_a(t - T_{spr,a}) \\
& + \frac{m_2}{(m_1+m_2+m_3)} (l_1 \sin\theta_a(t - T_{spr,a}) \\
& + r_2 \sin(\theta_a(t - T_{spr,a}) \\
& + \theta_k(t - T_{spr,k}))) + \frac{m_3}{(m_1+m_2+m_3)} \\
& \times (l_1 \sin\theta_a(t - T_{spr,a}) \\
& + l_2 \sin(\theta_a(t - T_{spr,a}) + \theta_k(t - T_{spr,k})) \\
& + r_3 \sin(\theta_a(t - T_{spr,a}) + \theta_k(t - T_{spr,k}) \\
& + \theta_h(t - T_{spr,h}))) \\
\approx\ & \frac{(m_1 r_1 + m_2(l_1 + r_2) + m_3(l_1 + l_2 + r_3))}{(m_1+m_2+m_3)} \theta_a \\
& \times (t - T_{spr,a}) \\
& + \frac{(m_2 r_2 + m_3 l_2)}{(m_1+m_2+m_3)} \theta_k(t - T_{spr,k}) \\
& + \frac{m_3 r_3}{(m_1+m_2+m_3)} \theta_h(t - T_{spr,h})
\end{aligned}$$

where $\theta_a$, $\theta_k$, and $\theta_h$ are ankle, knee, and hip joint angles of supporting leg, $m_i$ is the mass of each segment, $l_i$ is the length of each segment, and $r_i$ is the length from the distal end to the COM of each segment ($i$=1: lower leg, $i$=2: upper leg, $i$=3: trunk).

## Appendix B

Parameter values for simulation

- Muscle parameter
  $\alpha, \beta$, and $\gamma$ are set to be 0.11, 0.4, and 0.6 respectively.

$$\mathrm{A} = \begin{bmatrix} 0 & 0 & 0 & 0 & 0.023 & -0.036 & 0 & 0 & -0.040 \\ 0 & 0 & -0.040 & 0.049 & 0 & 0 & -0.025 & 0.049 & 0.050 \\ 0.132 & -0.092 & 0 & 0 & 0 & 0 & 0.049 & -0.054 & 0 \end{bmatrix}^{\mathrm{T}}$$

- Foot interaction to the ground
  $K_{gy} = 30000$, $B_{gy} = 500$, $K_{gx} = 10000$, $B_{gx} = 1000$;
  $\mu_k = 0.6$, $\mu_s = 1.2$.
  $y_{gy}(x) = 0$, which describes the flat ground.
- Spinal pattern generator

**Table 3** Parameters for periodic pattern generation

| | $u_{PG,1}$ | $u_{PG,2}$ | $u_{PG,3}$ | $u_{PG,4}$ |
|---|---|---|---|---|
| $\phi_i$ | 0.38 | 1.2 | 0.705 | 0.5275 |
| $h_i$ | $\cos(0.16\pi)$ | $\cos(0.2\pi)$ | $\cos(0.23\pi)$ | $\cos(0.125\pi)$ |

$$\mathrm{W}_{PG} = \begin{bmatrix} 0.3 & 0 & 0 & 0.8 & 0.76 & 0 & 0 & 0 & 0 \\ 0 & 0.38 & 0 & 0 & 0 & 0 & 0 & 0 & 0 \\ 0.4 & 0 & 0.64 & 0 & 0 & 0 & 0 & 0 & 0 \\ 0 & 0 & 0 & 0.8 & 0.9 & 0.4 & 0 & 0 & 0 \end{bmatrix}^{\mathrm{T}}$$

- Tactile receptor on the foot $\delta_F = 20$.
- Cerebrocerebellar system

$$\mathrm{I}_a = \begin{bmatrix} 0.2 & 0 \\ 0 & 1 \end{bmatrix}; \quad \mathrm{F}_2 = \begin{bmatrix} 0.6 & 0 \\ 0 & 0.3 \end{bmatrix};$$

$$\mathrm{I}_2 = \begin{bmatrix} 100 & 0 \\ 0 & 100 \end{bmatrix}; \quad \mathrm{I}_1 = 0; \quad gb_1 = 0, \quad gk_1 = 3;$$

$gb_2 = 0, gk_2 = 30.$

$$\mathrm{W}_C = \begin{bmatrix} 0 & 0 & 2 & -5 & 6 & -1 & 3 & -1 & -3 \\ 4 & -2.8 & 0 & 0 & 0 & 0 & 1.5 & -1.6 & 0 \end{bmatrix}^{\mathrm{T}}$$

- Estimates of $\hat{x}_{com}$, and $\hat{\theta}_{tr}$
  $p_{11} = 0.97$, $p_{21} = 0.53$, $p_{31} = 0.14$; $p_{12} = 1$, $p_{22} = -1$, $p_{32} = 1$.
- Spinal segmental inhibition

$$\theta_{th,a} = 0.35; \quad \theta_{th,k} = -0.35; \quad \theta_{th,h} = 0.55;$$

$$\mathrm{W}_{SR} = \rho \begin{bmatrix} 0 & 0 & 0 & 0 & 1 & 0 & 0 & 0 & 0 \\ 0 & 0 & 1 & 0 & 0 & 0 & 0 & 0 & 0 \\ 1 & 0 & 0 & 0 & 0 & 0 & 0 & 0 & 0 \end{bmatrix}^{\mathrm{T}}$$

where $\rho$ is a sufficient large number ($\rho > \eta_{PG}$).
- Initial conditions
  positions
  $\theta_1 = 0.2, \theta_3 = 0, \theta_5 = -0.2$ for right leg;
  $\theta_2 = 0, \theta_4 = -0.1, \theta_6 = 0.4$ for left leg.
  velocities
  $\dot{\theta}_1 = (f_{PG}+1)/2, \dot{\theta}_3 = -(f_{PG}+1)/2\,, \dot{\theta}_5 = (f_{PG}+1)/2$ for right leg;
  $\dot{\theta}_2 = -(f_{PG}+1)/2, \dot{\theta}_4 = (f_{PG}+1)/2, \dot{\theta}_6 = -(f_{PG}+1)/2$ for left leg.
- Reference signals
  $x_{com,ref} = 0.25$; $\theta_{tr,def} = 0$.

## References


Amstrong DM, Edgley SA (1988) Discharges of interpositus and Purkinje cells of the cat cerebellum during locomotion under different conditions. J Physiol 400:425–445

Anderson FC, Pandy MG (2001) Dynamic optimization of walking. J Biomech Eng 123:381–390

Baxendale RH, Ferrell WR (1981) The effect of knee joint afferent discharge on transmission in flexion reflex pathways in decerebrate cats. J Physiol (Lond) 315:231–242

Bizzi E et al (1992) Does the nervous system use equilibrium-point control to guide single and multiple joint movements? Behav Brain Sci. 15:603–613

Blaya J, Herr H (2004) Adaptive control of a variable-impedance ankle-foot orthosis to assist drop-foot gait. IEEE Trans Neural Sys Rehabil Eng 12(1):24–31

Brand RA et al (1986) The sensitivity of muscle force predictions to changes in physiological cross-sectional area. J Biomech 8:589–596

Bretzner F, Drew T (2005) Contribution of the motor cortex to the structure and the timing of hindlimb locomotion in the cat. J Neurophysiol 94(1):657–672

Brooke JD et al (1997) Sensori-sensory afferent conditioning with leg movement: gain control in spinal reflex and ascending paths. Prog Neurobiol 51:393–421

Cajigas-González I (2003) Linear control model of the spinal processing of descending neural signals. Master's Thesis, Elect Eng & Comp Sci, Massachusetts Institute of Technology

Calancie B et al (1994) Involuntary stepping after chronic spinal cord injury: Evidence for a central rhythm generator for locomotion in man. Brain 117:1143–1159

Capaday C et al (1999) Studies on the corticospinal control of human walking: I. Response to focal transcranial magnetic stimulation of the motor cortex. J Neurophysiol 81(1): 129–139
Cheung VC et al (2005) Central and sensory contributions to the activation and organization of muscle synergies during natural motor behaviors. J Neursci 25(27):6419–34
Christensen LO et al (2000) Cerebral activation during bicycle movements in man. Exp Brain Res 135(1):59–68
Collins JJ, Stewart I (1994) A group-theoretic approach to rings of coupled biological oscillators. Biol Cybern 71(2):95–103
Collins SH, Ruina A (2005) A bipedal walking robot with efficient and human-like gait. In: Proc IEEE Int Conf Robotics & Automation, Barcelona, Spain.
d'Avella A et al (2003) Combination of muscle synergies in natural motor behaviors. Nat Neurosci 6(3):300–308
d'Avella A, Bizzi E (2005) Shared and specific muscle synergies in natural motor behaviors. Proc Natl Acad Sci USA 102(8):3076–3081
Davis BL, Vaughan CL (1993) Phasive behavior of EMG signals during gait: Use of multivariate statistics. J EMG Kinesiol 3:51–60
Della Croce U et al (2001) A refined view of the determinants of gait. Gait Posture 14(2):79–84
Dimitrijevic MR et al (1998) Evidence for a spinal central pattern generator in humans. Ann NY Acad Sci 860:360–376
Dietz V (1992) Human neuronal control of automatic functional movements: interaction between central programs and afferent input. Physiol Rev 72(22):33–69
Dietz V, Harkema J (2004) Locomotor activity in spinal cord-injured persons. J Appl Physiol 96:1954–1960
Drew T (1993) Motor cortical activity during voluntary gait modifications in the cat. J Neurophysiol 70(1):179–199
Duysens J et al (2000) Loading-regulating mechanisms in gait and posture: comparative aspects. Physiol Rev 80(1):83–133
Flash T (1987) The control of hand equilibrium trajectories in multi-joint arm movements. Biol Cybern 57:257–274
Fledman AG (1986) Once more on the equilibrium trajectories in multi-joint arm movements. Biol Cybern 57:257–274
Freitas S et al (2006) Two kinematic synergies in voluntary whole-body movements during standing. J Neurophysiol 95: 636–645
Fuglevand AJ, Winter DA (1993) Models of recruitment and rate coding organization in motor-unit pools. J Neurophysiol 70(6):2470–2488
Fujita K, Sato H (1998) Intrinsic viscoelasticity of ankle joint during standing. In: Proceedings of the 20th annual international conference of the IEEE engineering in medicine and biology society 20(5):2343–2345
Fukuoka Y et al (2003) Adaptive dynamic walking of a quadruped robot on irregular terrain based on biological concepts. Int J Robot Res 22(3–4):187–202
Gilchrist LA, Winter DA (1997) A multisegment computer simulation of normal human gait, IEEE Trans Rehabil Eng 5(4):290–299
Grasso R et al (2004) Distributed plasticity of locomotor pattern generators in spinal cord injured patients. Brain 127(5):1019–1034
Grillner S (1975) Locomotion in vertebrates: central mechanisms and reflex interaction. Physiol Rev 55(2):247–304
Hiebert GW, Pearson KG (1999) Contribution of sensory feedback to the generation of extensor activity during walking in the decerebrate cat. J Neurophysiol 81:758–770
Hirai K et al (1998) The development of Honda humanoid robot. In: Proc the IEEE Int conf Robotic & Automation, Leuven, Belgium
Hofmann A (2006) Control rules for biomimetric human bipedal locomotion based on biomechanical principles. PhD Thesis, Elect Eng & Comp Sci, MIT
Hogan N (1985) The mechanics of multi-joint posture and movement control. Biol Cybern 52(5):315–331
Inman VT et al (1981) In: Lieberman JC (ed) Human walking. Williams & Wilkins, Balitimore pp. 41–55
Ivanenko YP et al (2004) Five basic muscle activation patterns account for muscle activity during human locomotion. J Physiol 556:267–282
Ivanenko YP et al (2006) Spinal cord maps of spatiotemporal alpha-motoneuron activation in humans walking at different speeds. J Neurophysiol 95:602–618
Iwasaki T, Zheng M (2006) Sensory feedback mechanism underlying entrainment of central pattern generator to mechanical resonance. Biol Cybern
Jo S, Massaquoi SG (2004) A model of cerebellum stabilized and scheduled hybrid long-loop control of upright balance. Biol Cybern 91:188–202
Johansson R et al (1988) Identification of human postural dynamics. IEEE Trans Biomed Eng 35(10):858–869
Kandel ER et al (2000) Principles of neural science, 4th edn. McGraw-Hill, New York
Katayama M, Kawato M (1993) Virtual trajectory and stiffness ellipse during multijoint arm movement predicted by neural inverse models. Biol Cybern 69:353–362
Kelly RM, Strick PL (2003) Cerebellar loops with motor cortex and prefrontal cortex of a nonhuman primate. J Neurosci 23:8432–8444
Kimura H et al (2001) Adaptive dynamic walking of a quadruped robot by using neural system model. Advanced robots 15(8):859–876
King WT (1927) Observations on the role of the cerebral cortex in the control of the postural reflex. Am J Physiol 80:311–326
Knikou M et al (2005) Modulation of flexion reflex induced by hip angle changes in human spinal cord injury. Exp Brain Res 164(4):577–586
Kriellaars DJ et al (1994) Mechanical entrainment of fictive locomotion in the decerebrate cat. J Neurophysiol 71(6):2074–2086
Kuo A (1995) An optimal control model for analyzing human postural balance. IEEE Trans Biomed Eng 42(1):87–101
Lacquaniti F et al (1999) Motor patterns in walking. News Physiol Sci 14:168–174
Lacquaniti F, Soechting JF (1986) Simulation studies on the control of posture and movement in a multi-jointed limb. Biol Cybern 54:367–378
Lam T, Pearson KG (2001) Proprioceptive modulation of hip flexor activity during the swing phase of locomotion in decerebrate cats. J Neurophysiol 86:1321–1332
Loram ID et al (2004) Paradoxical muscle movement in human standing. J Physiol 556.3:683–689
Massaquoi SG (1999) Modelling the function of the cerebellum in scheduled linear servo control of simple horizontal planar arm movements. PhD Thesis, Department of Electrical Engineering and Computer Science, MIT, Cambridge MA
Massaquoi SG, Hallett M (2002) Ataxia and other cerebellar syndromes. In: Jankovic, J, Tolosa, E (eds) Parkinson's desease and movement disorders. Williams & Wilkins, Baltimore pp. 523–686
Matsuoka K (1987) Mechanisms of frequency and pattern control in the neural rhythm generators. Biol Cybern 56:345–353
McGeer T (1993) Dynamics and control of bipedal locomotion. J Theor Biol 163(3):277–314
Mori S et al (2004) Integration of multiple motor segments for the elaboration of locomotion: role of the fastigial nucleus of the cerebellum. Prog Brain Res 143:341–351

Mori S et al (1999) Stimulation of a restricted region in the midline cerebellar white matter evokes coordinated quadrupedal locomotion in the decerebrate cat. J Neurophysiol 82(1): 290–300
Mori S et al (1998) Cerebellar-induced locomotion: reticulospinal control of spinal rhythm generating mechanism in cats. Ann N Y Acad Sci 860:94–105
Morton SM, Bastian AJ (2003) Relative contributions of balance and voluntary leg-coordination deficits to cerebellar gait ataxia. J Neurophyiol 89:1844–1856
Morton SM, Bastian AJ (2004) Cerebellar control of balance and locomotion. Neuroscientist 10(3):247–259
Nathan PW (1994) Effects on movement of surgical incisions into the human spinal cord. Brain 117(Pt2):337–346
Neptune RR et al (2004) Muscle mechanical work requirements during normal walking: the energetic cost of raising the body's center-of-mass is significant. J Biomech 37:817–825
Nielsen JB (2003) How we walk: central control of muscle activity during human walking. Neuroscientist 9(3):195–204
Ogihara N, Yamazaki N (2001) Generation of human bipedal locomotion by a bio-mimetic neuro-musculo-skeletal model. Biol Cybern 84:1–11
Olree KS, Vaughan CL (1995) Fundamental patterns of bilateral muscle activity in human locomotion. Biol Cybern 73:409–414
Osborn CE, Poppele RE (1992) Parallel distributed network characteristics of the DSCT, J Neurophysiol 68(4):1100–1112
Pandy MG, Berme N (1988) A numerical method for simulation the dynamics of human walking. J Biomech 21(12):1043–1051
Patla AE et al (1985) Model of a pattern generator for locomotion in mammals. Am J Physiol 248:R484–494
Perry J (1992) Gait analysis: normal and pathological function. McGraw-Hill, New York.
Peterka R (2003) Simplifying the complexities of maintaining balance. IEEE Eng Med Bio March (April):63–68
Peterson NT et al (1998) The effect of transcranial magnetic stimulation on the soleus H reflex during human walking. J Physiol (Lond) 513(Pt 2):599–610
Porter R, Lemon R (1993) Corticospinal function and voluntary movement. Oxford University Press, New York
Prentice SD, Drew T (2001) Contributions of the reticulospinal system to the postural adjustments occurring during voluntary gait modifications. J Neurophysiol 85(2):679–698
Ropper A, Brown RH (2005) Adams & Victor's principles of neurology. 8th edn. McGraw Hill Professional
Rossignol S et al (2006) Dynamic sensorimotor interactions in locomotion. Physiol Rev 86:89–154
Rudomin P, Schmidt RF (1999) Presynaptic inhibition in the vertebrate spinal cord revisited. Exp Brain Res 129(1):1–37
Saunders JB et al (1953) The major determinants in normal and pathological gait. J Bone & Joint Surgery 35A:543–558
Shik ML, Orlovsky GN (1976) Neurophysiology of locomotor automatism. Phsyiol Rev 56(3):465–501
Stein RB (1995) Presynaptic inhibition in humans, Prog in Neurobiol 47:533–544
Taga G (1995) A model of the neuro-musculo-skeletal system for human locomotion I. Emergence of basic gait. Biol Cybern 73:97–111
Tresch MC et al (1999) The construction of movement by the spinal cord. Nat Neurosci 2:162–167
Linde RQ (1999) Passive bipedal walking with phasic muscle contraction. Biol Cybern 81:227–237
Vukobratovic M et al (1990) Scientific fundamentals of robotics 7. Biped locomotion:dynamics stability, control and application. Springer, Berlin Heidelberg New York
Winter DA (1990) Biomechanics and motor control of human movement 2nd edn. Wiley, New York
Winter DA (1991) The biomechanics and motor control of human gait: normal, elderly and pathological. Waterloo Biomechanics Press, Waterloo
Winter DA (1995) Human balance and posture control during standing and walking. Gait & Posture 3:193–214
Winters JM (1995) How detailed should muscle models be to understand multi-joint movement coordination? Hum Mov Sci 14:401–442
Winters JM, Stark L (1985) Analysis of fundamental human movement patterns through the use of in-depth antagonistic muscle models. IEEE Trans Biomed Eng 32(10):820–839
Yang JF et al (2005) Split-belt treadmill stepping in infants suggests autonomous pattern generators for the left and right leg in humans. J Neurosci 25(29):6869–6876
Zajac FE (1989) Muscle and tendon: properties, models, scaling, and application to biomechanics and motor control. Critical Rev Biomed Eng 17(4):359–411
Zehr EP, Stein RB (1999) What functions do reflexes serve during human locomotion? Prog in Neurobiol 58:185–205
Zijlstra W et al (1998) Voluntary and involuntary adaptation of gait in Parkinson's disease. Gait & Posture 7(1):53–63